

AD-A072 764

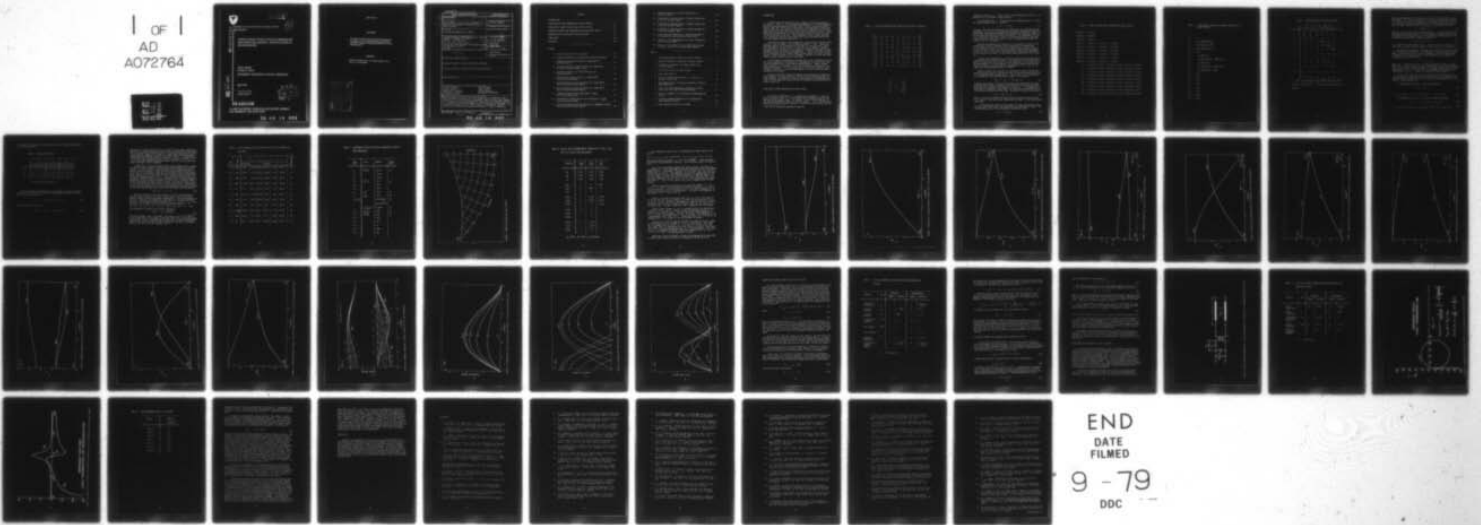
ARMY ELECTRONICS RESEARCH AND DEVELOPMENT COMMAND FO--ETC F/G 20/2  
ACOUSTIC WAVES IN CUBIC CRYSTALS: NETWORKS FOR SEMICONDUCTING V--ETC(U)  
APR 79 A BALLATO, C D BOSCO

UNCLASSIFIED

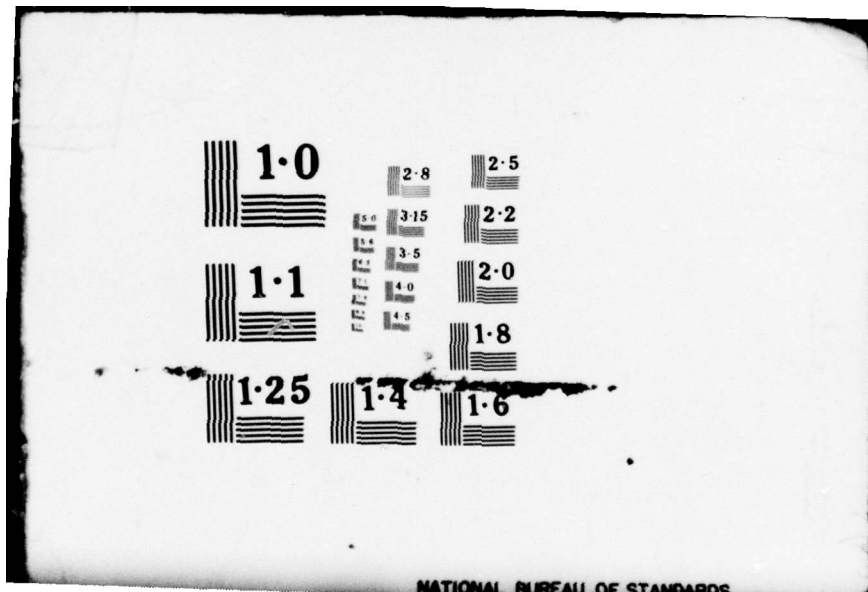
DELET-TR-79-9

NL

| OF |  
AD  
A072764



END  
DATE  
FILMED  
9 - 79  
DDC



NATIONAL BUREAU OF STANDARDS



LEVEL II

92

AD A072764

RESEARCH AND DEVELOPMENT TECHNICAL REPORT  
DELET-TR-79-9

ACOUSTIC WAVES IN CUBIC CRYSTALS: NETWORKS FOR  
SEMICONDUCTING VIBRATORS, AND APPLICATIONS TO  
GALLIUM ARSENIDE

Arthur Ballato  
Charles D. Bosco

ELECTRONICS TECHNOLOGY & DEVICES LABORATORY

April 1979

DISTRIBUTION STATEMENT  
Approved for public release;  
distribution unlimited.

DDC  
RECEIVED  
AUG 14 1979  
A

DDC FILE COPY

ERADCOM

US ARMY ELECTRONICS RESEARCH & DEVELOPMENT COMMAND  
FORT MONMOUTH, NEW JERSEY 07703

79 08 14 001

# NOTICES

## Disclaimers

The citation of trade names and names of manufacturers in this report is not to be construed as official Government indorsement or approval of commercial products or services referenced herein.

## Disposition

Destroy this report when it is no longer needed. Do not return it to the originator.

Accession For	
NTIS G&I	<input checked="" type="checkbox"/>
DDC TAB	
Unannounced	
Justification .	
By _____	
Distribution/	
Availability Codes	
Dist.	Avail and/or special
A	



## CONTENTS

INTRODUCTION . . . . .	1
PLANE ACOUSTIC WAVE PROPAGATION IN CUBIC CRYSTALS . . . . .	1
VIBRATIONS OF DOUBLY ROTATED CUBIC CRYSTAL PLATES . . . . .	29
EQUIVALENT NETWORK FOR SEMICONDUCTING PIEZOELECTRIC PLATES . . . . .	31
NONDESTRUCTIVE EVALUATION OF OXIDE LAYER MASS . . . . .	32
CONCLUSIONS . . . . .	39
REFERENCES . . . . .	40

FIGURES:

1. Primitive Region for Cubic Crystals . . . . .	12
2. Frequency Constants for $(YXw)\theta$ Cuts of Gallium Arsenide . . .	15
3. Piezoelectric Coupling Factors of $(YXw)\theta$ Cuts of Gallium Arsenide . . . . .	16
4. Direction Cosines of Particle Motion for $(YXw)\theta$ Cuts of Gallium Arsenide: Modes a and c . . . . .	17
5. Frequency Constants for $(YXw\ell) 45^\circ/\theta$ Cuts of Gallium Arsenide . . . . .	18
6. Piezoelectric Coupling Factors of $(YXw\ell) 45^\circ/\theta$ Cuts of Gallium Arsenide . . . . .	19
7. Direction Cosines of Particle Motion for $(YXw\ell) 45^\circ/\theta$ Cuts of Gallium Arsenide: Mode a . . . . .	20
8. Direction Cosines of Particle Motion for $(YXw\ell) 45^\circ/\theta$ Cuts of Gallium Arsenide: Mode b . . . . .	21
9. Frequency Constants for $(YXw\ell) \theta/\tan^{-1}(\sin\theta)$ Cuts of Gallium Arsenide . . . . .	22
10. Piezoelectric Coupling Factors of $(YXw\ell) \theta/\tan^{-1}(\sin\theta)$ Cuts of Gallium Arsenide . . . . .	23
11. Direction Cosines of Particle Motion for $(YXw\ell)\theta/\tan^{-1}(\sin\theta)$ Cuts of Gallium Arsenide: Mode a . . . . .	24

12.	Frequency Constants of Doubly Rotated Cuts of Gallium Arsenide . . . . .	25
13.	Piezoelectric Coupling Factors of Doubly Rotated Cuts of Gallium Arsenide: Mode a . . . . .	26
14.	Piezoelectric Coupling Factors of Doubly Rotated Cuts of Gallium Arsenide: Mode b . . . . .	27
15.	Piezoelectric Coupling Factors of Doubly Rotated Cuts of Gallium Arsenide: Mode c . . . . .	28
16.	Exact Equivalent Network for a Single Driven Mode in a Piezoelectric, Semiconducting Crystal Plate . . . . .	33
17.	Impedance Circle Representation of Lossy Transmission Line Equivalent Network . . . . .	35
18.	Reactance and Resistance versus Normalized Frequency for Lossy Transmission Line Equivalent Network . . . . .	36

TABLES:

1.	Elastopiezodielectric Matrix for Cubic Crystals . . . . .	2
2.	Rotated Piezoelectric Constants for Cubic Crystals . . . . .	4
3.	Piezoelectric Constants for Doubly Rotated Cuts of Cubic Crystals . . . . .	5
4.	Christoffel Matrix for Cubic Crystals . . . . .	6
5.	Force Density Matrix . . . . .	8
6.	Elastic Properties of Selected II - VI and III - V Crystals in Class $\bar{4}3m$ . . . . .	10
7.	Experimental Values for Physical Constants of GaAs at Room Temperature . . . . .	11
8.	Elastic and Electromechanical Properties of (100), (110), and (111) Cuts of Gallium Arsenide . . . . .	13
9.	Physical Parameters for Insulating and Semiconducting Crystals . . . . .	30
10.	Electrical Network Parameters for Insulating and Semiconducting Crystals . . . . .	34
11.	Room Temperature Densities of Oxides . . . . .	37

## INTRODUCTION

Prominent among the materials used in modern solid state technology are the III - V and II - VI semiconducting compounds.<sup>1-78\*</sup> These substances, typified by gallium arsenide, are most often of the zinc-blende structure, crystal class  $\bar{4}3m$ . Much work has been done on the growth and characterization of these crystals, because of their practical importance, to the point where high purity, high resistivity materials are becoming a reality. These compounds are piezoelectric in nature, but the effect is "short-circuited" if the resistivity is too low. The piezoelectric effect couples the electric and acoustic fields present within the crystal and makes possible devices that depend upon the interaction.<sup>1,2</sup>

The theory of acoustic wave propagation in piezoelectric semiconducting crystals is due to Kyame<sup>3</sup>, and to Hutson and White<sup>4</sup>. Arlt<sup>5</sup> gave an approximate analysis of semiconducting vibrators for the purpose of finding the piezoelectric coupling factor. Since that time a number of advances have been made in the theory of piezoelectric insulators, that have not been extended to cover the case of semiconductors<sup>6</sup>. These include the solution to the piezoelectrically coupled simple thickness modes of a plate vibrator, the use of doubly rotated cuts for resonators, synthesis of exact equivalent networks using transmission lines, and others.

In this report we undertake to explore some of the consequences of acoustic wave propagation in piezoelectric semiconductors of crystal class  $\bar{4}3m$  from the vantage point of the advances mentioned above. Doubly rotated plate vibrators are considered, as are coupled modes and transmission line equivalent networks. It is also shown how, by using such crystals as piezoelectric resonators, sensitive measurements of oxide films may be made in a nondestructive manner.

By way of providing practical examples of the properties of doubly rotated resonators of cubic materials, calculations have been made using gallium arsenide. This material is widely used because its wide bandgap provides for high temperature operation and its high mobility permits high frequency capability.

## PLANE ACOUSTIC WAVE PROPAGATION IN CUBIC CRYSTALS

The elastic stiffnesses  $c_{\lambda\mu}$ , piezoelectric constants  $e_{i\lambda}$ , and dielectric permittivities  $\epsilon_{ij}$  of insulating crystals depend, for their symmetries, on the crystal class. For crystals in cubic classes  $\bar{4}3m$  and  $23$ , the elastopiezodielectric matrix is given in Table 1. It is seen that these materials are dielectrically isotropic; in addition, they have only one pie-

\* See list of references beginning on page 40.

TABLE 1. ELASTOPIEZODIELECTRIC MATRIX FOR CUBIC CRYSTALS.

$$\begin{bmatrix}
 11 & 12 & 12 & 0 & 0 & 0 & | & 0 & 0 & 0 \\
 12 & 11 & 12 & 0 & 0 & 0 & | & 0 & 0 & 0 \\
 12 & 12 & 11 & 0 & 0 & 0 & | & 0 & 0 & 0 \\
 0 & 0 & 0 & 44 & 0 & 0 & | & 14 & 0 & 0 \\
 0 & 0 & 0 & 0 & 44 & 0 & | & 0 & 14 & 0 \\
 0 & 0 & 0 & 0 & 0 & 44 & | & 0 & 0 & 14 \\
 \hline
 0 & 0 & 0 & 14 & 0 & 0 & | & 11 & 0 & 0 \\
 0 & 0 & 0 & 0 & 14 & 0 & | & 0 & 11 & 0 \\
 0 & 0 & 0 & 0 & 0 & 14 & | & 0 & 0 & 11
 \end{bmatrix}$$

$$\begin{bmatrix}
 c^E & | & e_t \\
 \hline
 e & | & \epsilon^s
 \end{bmatrix}$$

zoelectric constant,  $e_{14}$ , which reduces the transformation of the  $e_{i\lambda}$  for rotated axes to a problem in simple geometry.

For coordinate axes  $X'_i$  transformed by an orthogonal matrix  $\alpha_{ij}$  from the crystallographic axes  $X_j$  we have

$$X'_i = \alpha_{ij} X_j \quad (1)$$

In Table 2 the left-hand entries are the subscripts ( $k\mu$ ) representing the quantities ( $e'_{k\mu}/e_{14}$ ), the normalized transformed piezoelectric constants; the numbers in parentheses preceding the constants are numerical factors. On the right-hand side are products consisting of  $\alpha_{ij}$  components; only the ( $ij$ ) subscripts are written. Table 2 follows from writing out the transformation law for tensors of the third rank, and applying the simplifications in the  $e_{i\lambda}$  from Table 1.

When the transformation of Equation (1) is expressed in terms of the angles  $\phi$  and  $\theta$  used to describe doubly rotated cuts of orientation<sup>7</sup> ( $YX\omega\ell$ ) $\phi/\theta$ , the result is the further simplification shown in Table 3. On the left-hand side are the indices representing the transformed quantities ( $e_{k\mu}/e_{14}$ ), and on the right-hand side are the angular dependencies of these quantities; numbers in parentheses denote equalities, e.g.,  $e'_{36} = e_{14}$ .

Acoustic wave propagation in an arbitrary direction in crystals may be calculated by the Christoffel method<sup>6</sup>. The direction of plane wave propagation is taken to be the  $X'_2$  axis, and the quantities  $\alpha_{2i}$  in Equation (1) are abbreviated  $\alpha_i$  in the following. The elastic, piezoelectric and dielectric constants are transformed to the quantities  $\Gamma$ ,  $\Xi$ , and  $\epsilon$ , respectively, by the relations given in Table 4.

When an acoustic wave travels in a piezoelectric medium, the motions produce internal electric fields which serve to increase the effective elastic constant governing the wave motion. This effect is called "piezoelectric stiffening"; the stiffened elastic moduli  $\bar{\Gamma}$  are given by

$$\bar{\Gamma}_{jk} = \Gamma_{jk} + \Xi_j \Xi_k / \epsilon \quad (2)$$

The  $\bar{\Gamma}$  are the elements of a secular determinant that determines the three stiffened modal elastic constants  $\bar{\alpha}_m$  for the three types of plane acoustic waves that can propagate in the assumed direction  $X'_2$ . Associated with each mode are orthonormal eigenvectors  $\gamma_m$  that give the directions of particle motion associated with each mode. The modes are ordered according to

$$\bar{\alpha}_a > \bar{\alpha}_b \geq \bar{\alpha}_c \quad (3)$$

Mode a is the quasi-longitudinal mode, with particle motion nearly along  $X'_2$ ; mode b is the faster quasi-shear mode, and mode c is the slower quasi-shear mode.

The semiconducting nature of the crystal is taken into account by permitting current terms other than displacement and piezoelectric flows. The current density due to drift introduces a conductivity term<sup>3</sup>

$$J_i = \sigma_{ij} E_j \quad (4)$$

TABLE 2. ROTATED PIEZOELECTRIC CONSTANTS FOR CUBIC CRYSTALS

$$(1/6) \cdot 11 = 12 \cdot 13 \cdot 11$$

$$(1/6) \cdot 22 = 22 \cdot 23 \cdot 21$$

$$(1/6) \cdot 33 = 32 \cdot 33 \cdot 31$$

$$(1/2) \cdot 12 = 22 \cdot 23 \cdot 11 + 21 \cdot 23 \cdot 12 + 21 \cdot 22 \cdot 13$$

$$(1/2) \cdot 13 = 32 \cdot 33 \cdot 11 + 31 \cdot 33 \cdot 12 + 31 \cdot 32 \cdot 13$$

$$(1/2) \cdot 21 = 12 \cdot 13 \cdot 21 + 11 \cdot 13 \cdot 22 + 11 \cdot 12 \cdot 23$$

$$(1/2) \cdot 23 = 32 \cdot 33 \cdot 21 + 31 \cdot 33 \cdot 22 + 31 \cdot 32 \cdot 23$$

$$(1/2) \cdot 31 = 12 \cdot 13 \cdot 31 + 11 \cdot 13 \cdot 32 + 11 \cdot 12 \cdot 33$$

$$(1/2) \cdot 32 = 22 \cdot 23 \cdot 31 + 21 \cdot 23 \cdot 32 + 21 \cdot 22 \cdot 33$$

$$14 = 11 \cdot (22 \cdot 33 + 23 \cdot 32) + 12 \cdot (23 \cdot 31 + 21 \cdot 33) + 13 \cdot (21 \cdot 32 + 22 \cdot 31)$$

$$15 = 11 \cdot (32 \cdot 13 + 33 \cdot 12) + 12 \cdot (33 \cdot 11 + 31 \cdot 13) + 13 \cdot (31 \cdot 12 + 32 \cdot 11)$$

$$16 = 11 \cdot (12 \cdot 23 + 13 \cdot 22) + 12 \cdot (13 \cdot 21 + 11 \cdot 23) + 13 \cdot (11 \cdot 22 + 12 \cdot 21)$$

$$24 = 21 \cdot (22 \cdot 33 + 23 \cdot 32) + 22 \cdot (23 \cdot 31 + 21 \cdot 33) + 23 \cdot (21 \cdot 32 + 22 \cdot 31)$$

$$25 = 21 \cdot (32 \cdot 13 + 33 \cdot 12) + 22 \cdot (33 \cdot 11 + 31 \cdot 13) + 23 \cdot (31 \cdot 12 + 32 \cdot 11)$$

$$26 = 21 \cdot (12 \cdot 23 + 13 \cdot 22) + 22 \cdot (13 \cdot 21 + 11 \cdot 23) + 23 \cdot (11 \cdot 22 + 12 \cdot 21)$$

$$34 = 31 \cdot (22 \cdot 33 + 23 \cdot 32) + 32 \cdot (23 \cdot 31 + 21 \cdot 33) + 33 \cdot (21 \cdot 32 + 22 \cdot 31)$$

$$35 = 31 \cdot (32 \cdot 13 + 33 \cdot 12) + 32 \cdot (33 \cdot 11 + 31 \cdot 13) + 33 \cdot (31 \cdot 12 + 32 \cdot 11)$$

$$36 = 31 \cdot (12 \cdot 23 + 13 \cdot 22) + 32 \cdot (13 \cdot 21 + 11 \cdot 23) + 33 \cdot (11 \cdot 22 + 12 \cdot 21)$$

TABLE 3. PIEZOELECTRIC CONSTANTS FOR DOUBLY ROTATED CUTS OF CUBIC CRYSTALS.

11	=	0
22	=	$-3 \cdot \sin 2\theta \cdot \cos^2 \theta \cdot \sin \theta$
33	=	$-3 \cdot \sin 2\theta \cdot \cos \theta \cdot \sin^2 \theta$
12	=	$+2 \cdot \cos 2\theta \cdot \cos \theta \cdot \sin \theta$
13	=	$-(12)$
21	=	$\sin 2\theta \cdot \sin \theta$
23	=	$\sin 2\theta \cdot (2 \cdot \cos^2 \theta - \sin^2 \theta) \cdot \sin \theta$
31	=	$\sin 2\theta \cdot \cos \theta$
32	=	$\sin 2\theta \cdot (2 \cdot \sin^2 \theta - \cos^2 \theta) \cdot \cos \theta$
14	=	$\cos 2\theta \cdot (\cos^2 \theta - \sin^2 \theta)$
15	=	(31)
16	=	(21)
24	=	(32)
25	=	(14)
26	=	(12)
34	=	(23)
35	=	$-(12)$
36	=	(14)

TABLE 4. CHRISTOFFEL MATRIX FOR CUBIC CRYSTALS.

	$\alpha_1^2$	$\alpha_2^2$	$\alpha_3^2$	$\alpha_2 \alpha_3$	$\alpha_3 \alpha_1$	$\alpha_1 \alpha_2$
$\Gamma_{11}$	11	44	44	0	0	0
$\Gamma_{22}$	44	11	44	0	0	0
$\Gamma_{33}$	44	44	11	0	0	0
$\Gamma_{23}$	0	0	0	12+44	0	0
$\Gamma_{31}$	0	0	0	0	12+44	0
$\Gamma_{12}$	0	0	0	0	0	12+44
$\Xi_1$	0	0	0	2·14	0	0
$\Xi_2$	0	0	0	0	2·14	0
$\Xi_3$	0	0	0	0	0	2·14
$\epsilon$	11	11	11	0	0	0

$\Gamma_{ik}$  and  $\epsilon$  for classes 23, 432, m3,  $\bar{4}3m$ , and m3m;  $\Xi_1$  for classes 23 and  $\bar{4}3m$ ; all  $\Xi_i$  are zero for classes 432, m3, and m3m.

while a term depending on charge carrier gradients will contribute a diffusion term<sup>4</sup>. If  $\sigma$  is finite, the effect is to make  $\epsilon$  complex; the addition of a diffusion term does not change this situation, but makes the relation more involved. Because of the piezoelectric stiffening expressed in Equation (2), when  $\epsilon$  becomes complex, so does  $\bar{c}_m$ , and the modal velocities

$$v_m = \sqrt{\bar{c}_m / \rho} , \quad (5)$$

where  $\rho$  is the mass density, also become complex. This means that the waves are attenuated as they progress. The piezoelectric constants are only influenced to a minor extent because the  $\gamma_m$  eigenvectors become complex, and the effective piezoelectric constant for mode  $m$  is

$$e_m = \gamma_{mj} \bar{\Xi}_j . \quad (6)$$

If, in addition to modifications to  $\epsilon$ , viscous forces are included,<sup>3,6,8</sup> the effect is to add a further imaginary term to the elastic stiffnesses  $\bar{c}_m$ .

The effective piezoelectric constant  $e_m$  in Equation (6) holds for electric fields directed along  $X'_2$ . For generation of surface acoustic waves<sup>9</sup> (SAW) or shallow bulk acoustic waves<sup>10</sup> (SBAW) excited via interdigitated electrodes<sup>9</sup>, the piezoelectrically induced mechanical force densities  $F_j$  are determined from the relation

$$F_j = - e_{kij} E_{k,i} \quad (7)$$

where  $E_{k,i}$  stands for  $\partial E_k / \partial x_i$ , and the uncontracted indices on  $e$  have been used.<sup>11</sup> Table 5 gives the force density matrix for crystal classes  $\bar{4}3m$  and 23, using the  $e'$  entries from Table 3 for doubly rotated cuts; only the subscripts are shown. One may see that the symmetry present permits the substitution  $E_{j,k} = E_{k,j}$  as well as a number of other relations.

As far as the purely acoustic wave velocities of SAW propagation on cubic substrates is concerned, explicit formulas can only be given for propagation along the cube axis  $[100]$  and along the face diagonal  $[110]$  directions. The expressions are:<sup>12</sup>

For propagation along  $[100]$ , with the abbreviation

$$R = \rho v^2 / c_{11} , \quad (8)$$

$$(1 - c_{11} R / c_{44}) \cdot (1 - R - c_{12}^2 / c_{11}^2)^2 = R^2 (1 - R) . \quad (9)$$

For propagation along  $[110]$ , with the further abbreviation

$$c_o = (c_{11} + c_{12} + 2 c_{44}) / 2 , \quad (10)$$

$$(1 - c_{11} R / c_{44}) \cdot ((c_{11} c_o - c_{12}^2) / c_{11}^2 - R)^2 = R^2 (c_o / c_{11} - R) . \quad (11)$$

In Equations (9) and (11), the single real root for R yields the SAW velocity v from Equation (8).

TABLE 5. FORCE DENSITY MATRIX.

	E <sub>1</sub>			E <sub>2</sub>			E <sub>3</sub>		
	E <sub>1,1</sub>	E <sub>1,2</sub>	E <sub>1,3</sub>	E <sub>2,1</sub>	E <sub>2,2</sub>	E <sub>2,3</sub>	E <sub>3,1</sub>	E <sub>3,2</sub>	E <sub>3,3</sub>
-F <sub>1</sub>	0	21	31	21	12	14	31	14	-12
-F <sub>2</sub>	21	12	14	12	22	32	14	32	23
-F <sub>3</sub>	31	14	-12	14	32	23	-12	23	33

Crystal classes  $\bar{4}3m$  and 23.

Table 6 presents representative values of elastic constants and mass densities for selected II - VI and III - V compounds, along with the anisotropy ratios, A, defined as

$$A = 2 \kappa_{44} / (\kappa_{11} - \kappa_{12}), \quad (12)$$

and the bulk moduli, defined as

$$B = (\kappa_{11} + 2 \kappa_{12}) / 3. \quad (13)$$

The values of A and B for the entries in Table 6 do not differ appreciably. Because of its high technological interest gallium arsenide has been selected to illustrate some of the foregoing. Its physical properties are fairly representative of members in crystal class  $\bar{4}3m$ . Some of the experimental values characterizing this material are given in Table 7. In the table,  $T_c$  is the first order temperature coefficient of the elastic stiffness,  $\alpha^{(1)}$  is the first order thermal expansion constant, and the  $c_{\lambda\mu\nu}$  are the third order (nonlinear) elastic constants.

By making use of the Christoffel method sketched above one may compute the acoustic and piezoelectric properties for wave propagation in any direction. For cubic crystals, three directions are of primary importance from the point of geometry. These are the  $[100]$  direction (along the cube axis), the  $[110]$  direction (along the face diagonal; normal to the dodecahedral planes (110), and the  $[111]$  direction (along the body diagonal; normal to the octahedral planes (111)). These principal directions are not necessarily the directions of greatest interest as far as device designs are concerned, but they do bound the primitive region, the irreducible  $1/48$ th of the unit sphere, for these crystal classes. The region is shown in Figure 1, in polar coordinates, in terms of the angles  $\phi$  and  $\theta$ ; the constant  $\theta$  paths are portions of circles, the constant  $\phi$  paths are portions of radii, and the line drawn between the  $[100]$  and  $[111]$  directions has the equation

$$\tan \theta = \sin \phi. \quad (14)$$

Numerical values for  $N_m = \sigma_m/2$ ,  $|k_m|$  and  $|g_{mi}|$  for high resistivity GaAs are given in Table 8 for (100), (110), and (111) cuts; the entries marked by dashes indicate eigenvector degeneracies. For wave propagation in the  $[100]$  direction, corresponding to the (100) cut, the modes are piezoinactive. The effective elastic constants are  $c_a = c_{11}$ ,  $c_b = c_c = c_{44}$ . Corresponding to the (110) cut are the effective elastic values

$$c_a = c_{44} + (c_{11} + c_{12})/2, \quad \bar{c}_b = \bar{c}_{44} = c_{44} + e_{14}^2/\epsilon, \quad \text{and} \quad c_c = (c_{11} - c_{12})/2.$$

The piezoelectric coupling coefficients, defined by

$$|k_m| = |e_m| / \sqrt{\bar{c}_m \epsilon}, \quad (15)$$

are zero for modes a and c; for mode b the value is  $|k_b| = |e_{14}| / \sqrt{\bar{c}_{44} \epsilon}$ . As seen from Table 8, the b mode is polarized along  $[001]$ , the a mode along  $[110]$  and the c mode is perpendicular to both; the  $[110]$  axis has particle motion either strictly along the phase progression direction, or perpendicular to it, and is thus an "acoustic" axis.<sup>27</sup>

TABLE 6. ELASTIC PROPERTIES OF SELECTED II-VI and III-V CRYSTALS IN CLASS  $\bar{4}3m$ .

Type	Crystal	$\rho$	$c_{11}$	$c_{12}$	$c_{44}$	A	B	Reference
		$10^{+3}\text{kg/m}^3$	$10^{+9}\text{Pa}$					
3-5	AlSb	3.460	89.39	44.27	41.55	1.84	59.31	13
2-6	CdTe	5.840	53.51	36.81	19.94	2.39	42.38	14
3-5	GaSb	5.619	88.39	40.33	43.16	1.80	56.35	15
3-5	GaAs	5.3169	118.77	53.72	59.44	1.83	75.40	16
3-5	GaP	4.13	141.2	62.53	70.47	1.79	88.75	17
3-5	InSb	5.7747	67.00	36.49	30.19	1.98	46.66	18
3-5	InAs	5.70	83.29	45.26	39.59	2.08	57.94	19
2-6	ZnSe	5.262	81.0	48.8	44.1	2.74	59.53	20
2-6	ZnS( $\beta$ )	4.088	104.6	65.3	46.13	2.35	78.40	20
2-6	ZnTe	5.636	71.3	40.7	31.2	2.04	50.90	20
3-5	InP	4.78	102.2	57.6	46.00	2.06	72.47	21

TABLE 7. EXPERIMENTAL VALUES FOR PHYSICAL CONSTANTS OF GaAs AT ROOM TEMPERATURE.

Quantity	Unit	Numeric	Reference
$c_{11}$	$10^{+9}$ Pa	118.77	16
$c_{12}$		53.72	
$c_{44}$		59.44	
$Tc_{11}$	$10^{-6}$ /K	-152.	22
$Tc_{12}$		-287.	
$Tc_{44}$		-37.8	
$e_{14}$	C/m <sup>2</sup>	-0.16	23
$\epsilon_{11}$	pF/m	116.7	24
$\epsilon_{11}(T)/\epsilon_0$	-	12.73(1+ $\beta$ T)	24
		$\beta=1.2 \times 10^{-4}$ /K	
$\rho$	$10^{+3}$ kg/m <sup>3</sup>	5.3169	16
$\alpha(1)$	$10^{-6}$ /K	6.86	25
$c_{111}$	$10^{+9}$ Pa	-622.	26
$c_{112}$		-387.	
$c_{123}$		-57.	
$c_{144}$		+2.	
$c_{166}$		-269.	
$c_{456}$		-39.	

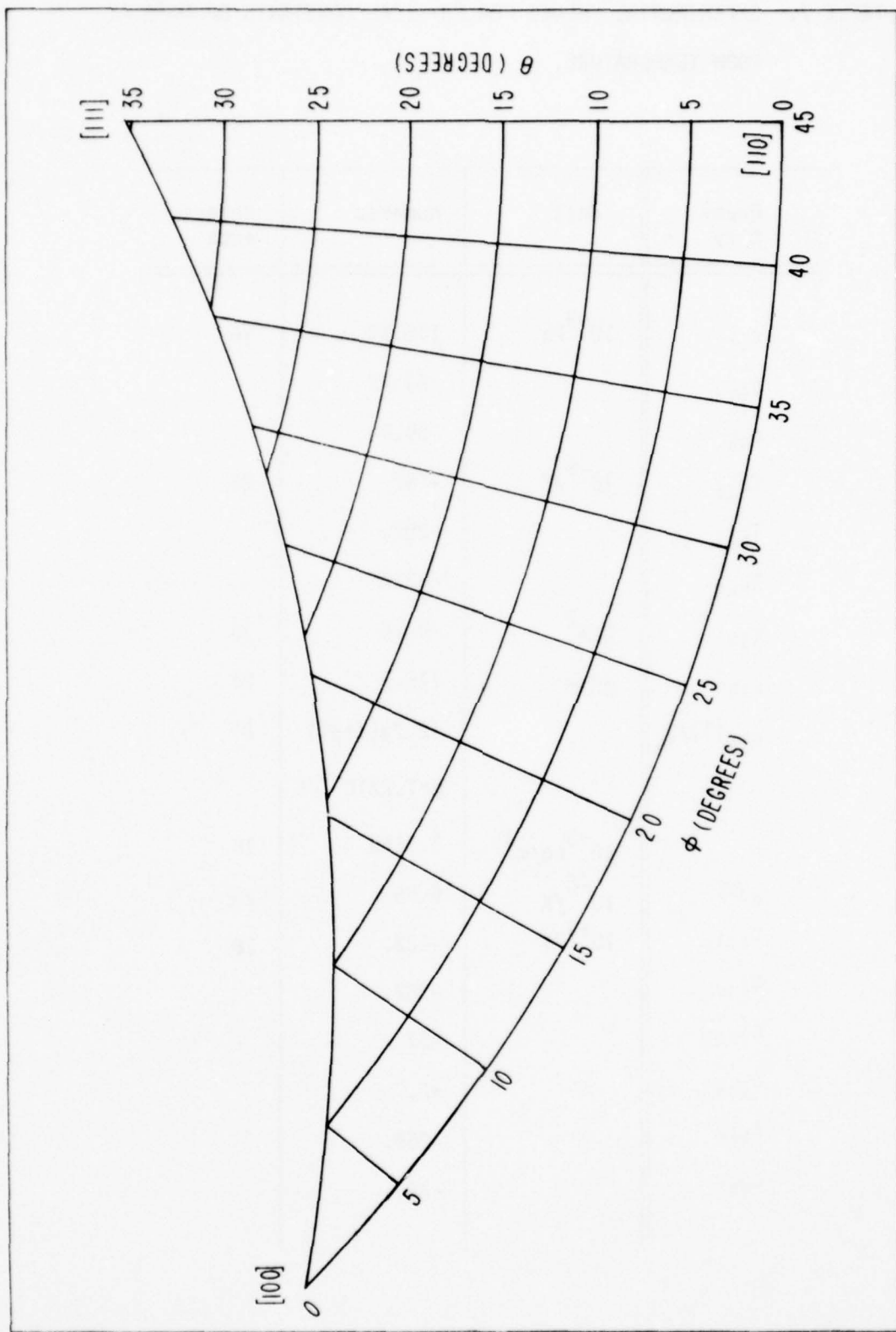


FIGURE 1. PRIMITIVE REGION FOR CUBIC CRYSTALS.

TABLE 8. ELASTIC AND ELECTROMECHANICAL PROPERTIES OF (100), (110),  
AND (111) CUTS OF GALLIUM ARSENIDE.

Quantity	(100) Cut	(110) Cut	(111) Cut
$N_a$	2.363	2.617	2.699
$N_b$	1.672	1.672	1.397
$N_c$	1.672	1.237	1.397
$ k_a $	0	0	4.34
$ k_b $	0	6.08	0
$ k_c $	0	0	0
$ \gamma_{a1} $	1	$1/\sqrt{2}$	$1/\sqrt{3}$
$ \gamma_{a2} $	0	$1/\sqrt{2}$	$1/\sqrt{3}$
$ \gamma_{a3} $	0	0	$1/\sqrt{3}$
$ \gamma_{b1} $	0	0	-
$ \gamma_{b2} $	-	0	-
$ \gamma_{b3} $	-	1	-
$ \gamma_{c1} $	0	$1/\sqrt{2}$	-
$ \gamma_{c2} $	-	$1/\sqrt{2}$	-
$ \gamma_{c3} $	-	0	-

$N_m$  in MHz - mm = km/s;  $k_m$  in percent.

Wave propagation along [111] is characterized by modal elastic stiffnesses

$$\bar{c}_a = (c_{11} + 2c_{12} + 4c_{44} + 4e_{14}^2/\epsilon)/3, \quad c_b = c_c = (c_{11} + c_{44} - c_{12})/3.$$

The coupling factor for mode a is  $|k_a| = |2e_{14}|/\sqrt{3\bar{c}_a\epsilon}$ , while the other modes have zero piezoelectric coupling. This direction is also an "acoustic" axis.

Cuts of GaAs intermediate between the three principal directions are considered next. First, the great circle path from [100] to [110] with  $\theta=0^\circ, 0^\circ \leq \phi \leq 45^\circ$ , denoted path I, is described. Figures 2, 3, and 4 give  $N_m$ ,  $|k_m|$ , and  $|\gamma_m|$ , respectively, for path I. The degeneracy in the b and c modes that exists at [100] is broken as soon as this specific direction is departed from, so, for the path chosen, the  $|\gamma_m|$  may be extrapolated back to the end point. For this path, therefore, one has  $|\gamma_b| = (0, 0, 1)$ ; this vector does not change during path I.  $|\gamma_c|$  is the same as  $|\gamma_a|$  with a renumbering of the components.

Path II, consisting of the great circle path with angles  $\phi = 45^\circ, 0^\circ \leq \theta \leq \sin^{-1}(1/\sqrt{3})$ , produces the results shown in Figures 5, 6, 7, and 8. This path starts at [110] and ends at [111]; the latter degeneracy is removed, as described above, by extrapolation. For mode c, the components do not change:  $|\gamma_c| = (1/\sqrt{2}, 1/\sqrt{2}, 0)$ .

Path III, the great circle path from [100] to [111], has angles of  $0^\circ \leq \phi \leq 45^\circ, \theta = \tan^{-1}(\sin\phi)$ . Figures 9, 10, and 11 give the values for  $N_m$ ,  $|k_m|$  and  $|\gamma_a|$  for this path. The behavior of  $|\gamma_b|$  for path III is exactly as that of  $|\gamma_b|$  for path II, shown in Figure 8, and  $|\gamma_c|$  for path III is the same as  $|\gamma_a|$  for path I when the 1 and 2 components are interchanged.

General doubly rotated cuts of high resistivity GaAs are considered in Figures 12, 13, 14, and 15. Figure 12 gives the frequency constants  $N_m$  versus  $\theta$  for various  $\phi$  values. One sees the b and c mode degeneracy at  $\theta = \sin^{-1}(1/\sqrt{3})$ , corresponding to [111]. Of interest is the behavior of the c mode between  $28.78^\circ$  and  $28.79^\circ$ , where the value of  $N_c$  is virtually independent of  $\phi$ ; this appears to be an accidental occurrence.

Figures 13, 14, and 15 show the piezoelectric coupling factors, computed from Equation (15), for modes a, b, and c, respectively. The a mode has its maximum value at  $\phi=45^\circ, \theta = \sin^{-1}(1/\sqrt{3})$ , i.e., at the (111) cut. The b mode value is a maximum for the (110) cut at  $\phi=45^\circ, \theta=0^\circ$ ; this drops off as  $\theta$  is increased, and becomes zero at  $\sin^{-1}(1/\sqrt{3})$  and beyond. The c mode behaves in a complementary manner, with zero coupling for  $\phi=45^\circ$  and  $\theta \leq \sin^{-1}(1/\sqrt{3})$ , rising beyond this  $\theta$  value.

Additional details relating to acoustic wave propagation in cubic and/or other crystal classes are given in References 28 to 44, and 69-78.

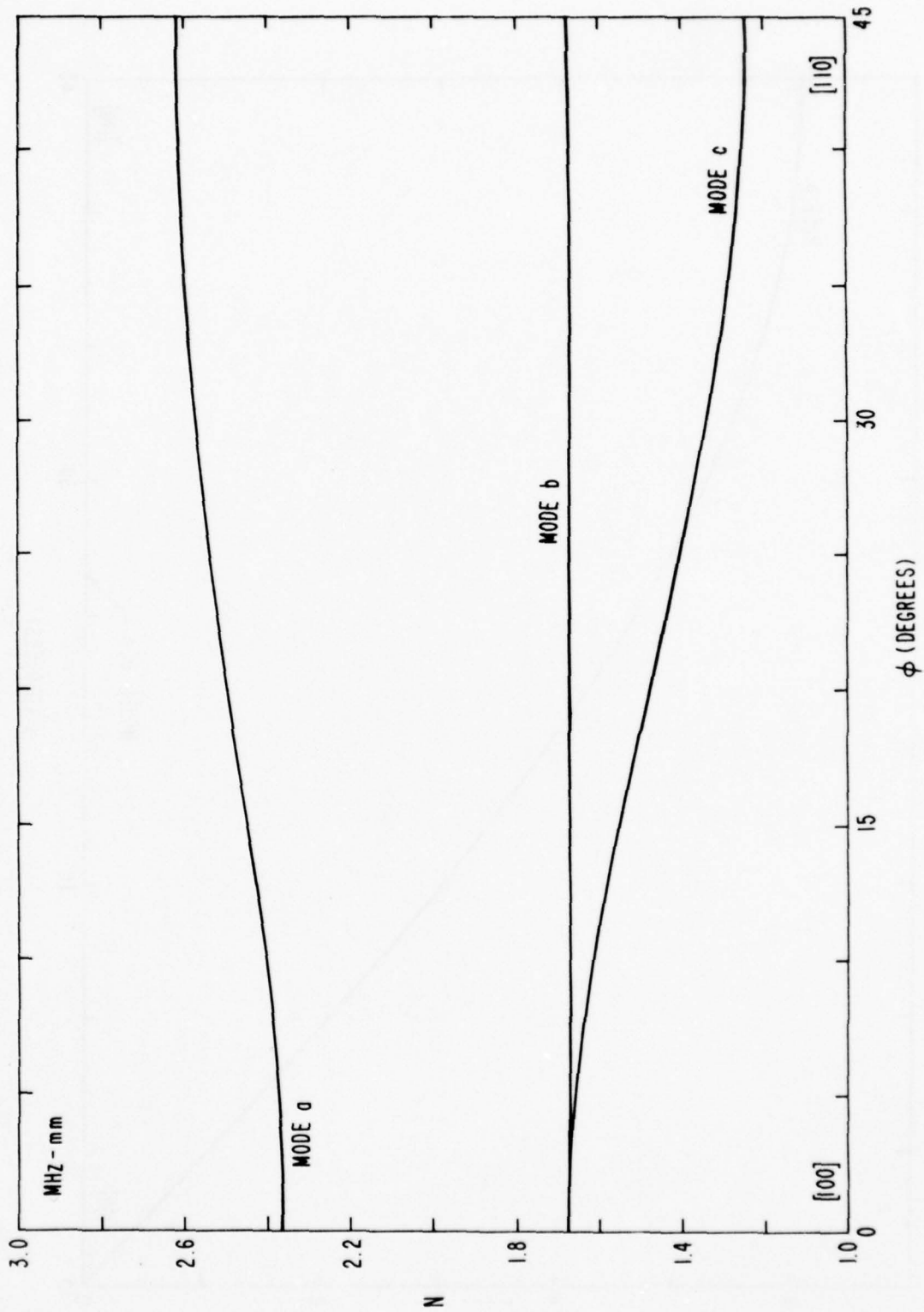


FIGURE 2. FREQUENCY CONSTANTS FOR  $(YX_w)\phi$  CUTS OF GALLIUM ARSENIDE.

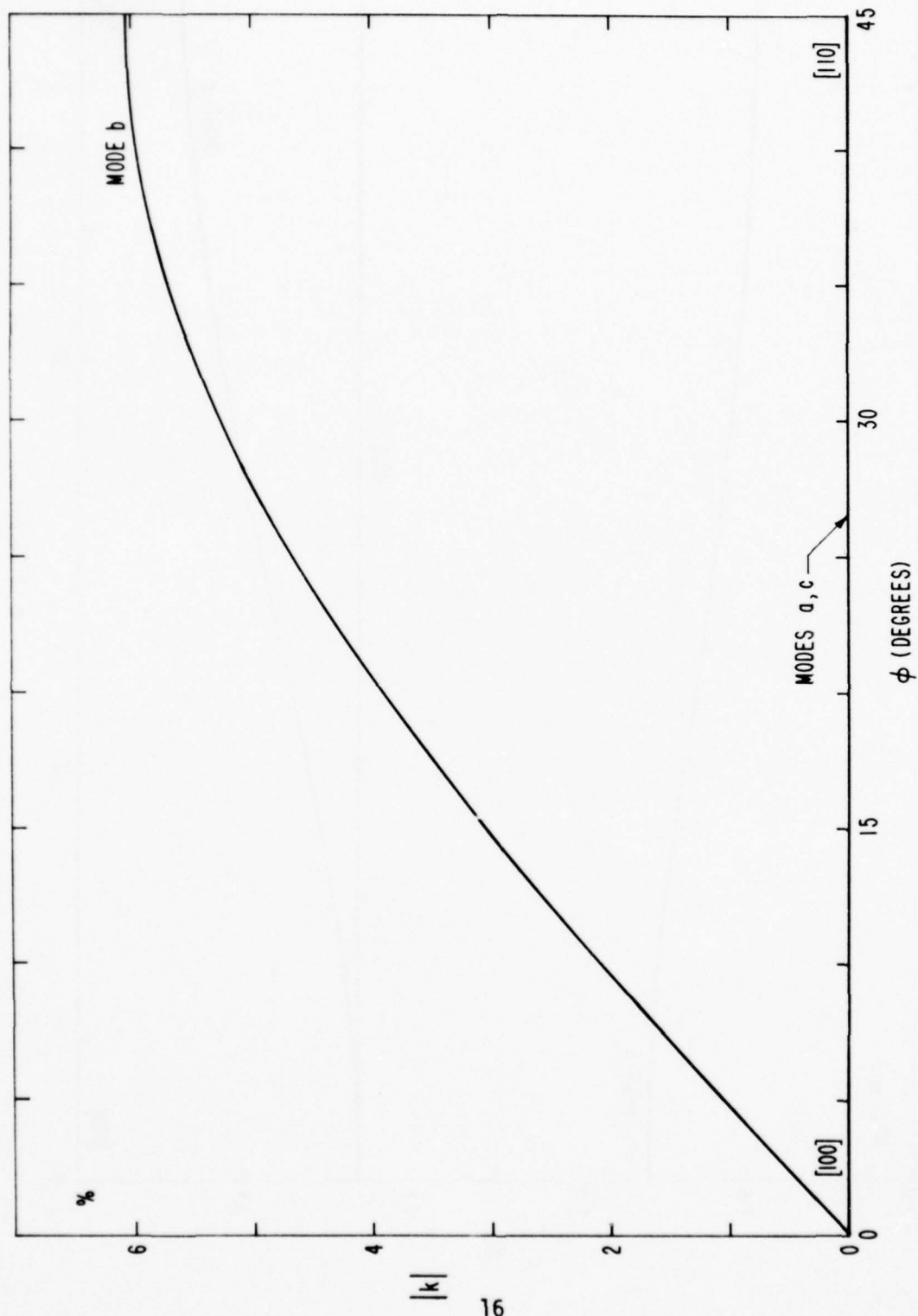


FIGURE 3. PIEZOELECTRIC COUPLING FACTORS OF (YXw) $\phi$  CUTS OF GALLIUM ARSENIIDE.

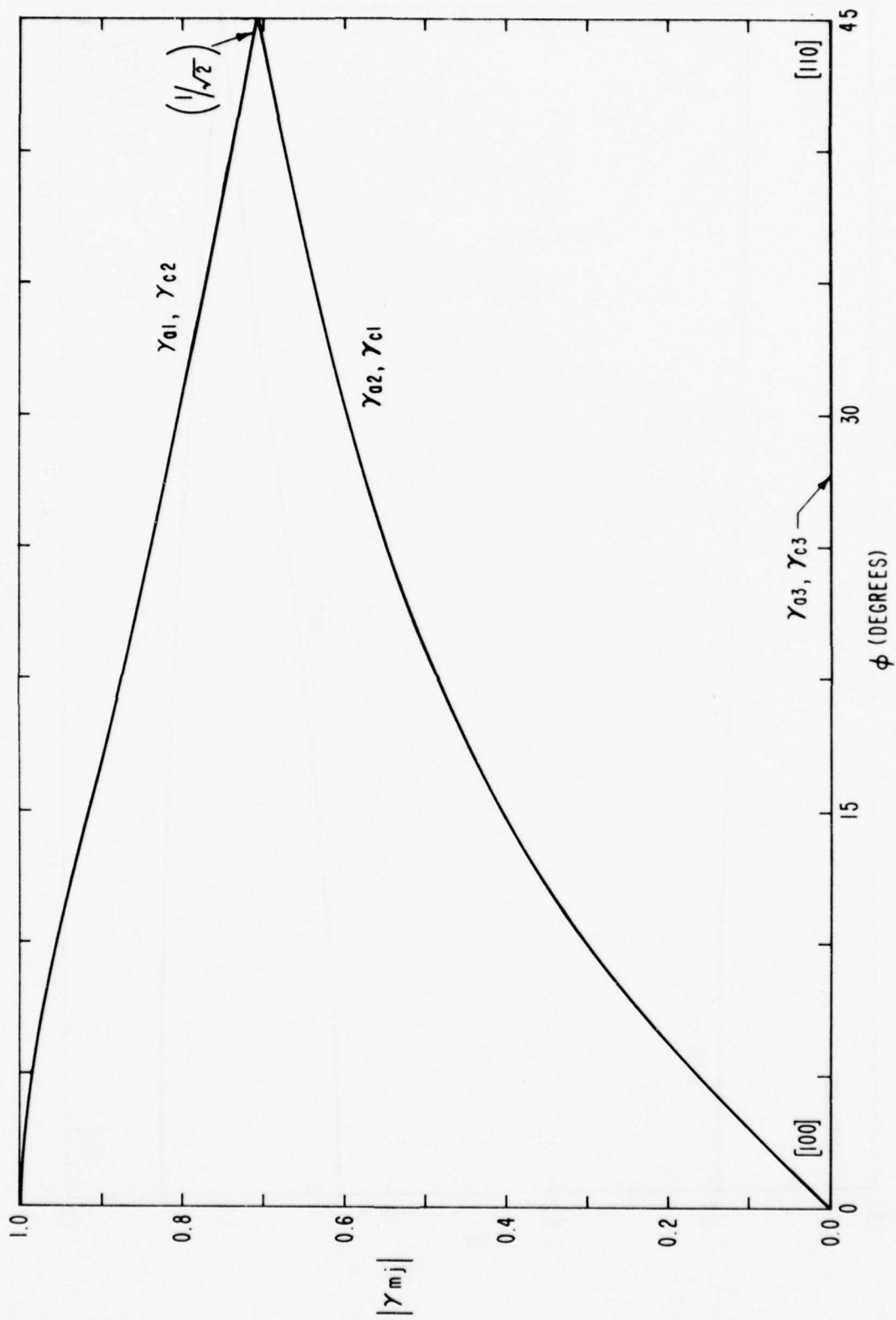


FIGURE 4. DIRECTION COSINES OF PARTICLE MOTION FOR  $(YX_w)\phi$  CUTS OF GALLIUM ARSENIIDE: MODES a AND c.

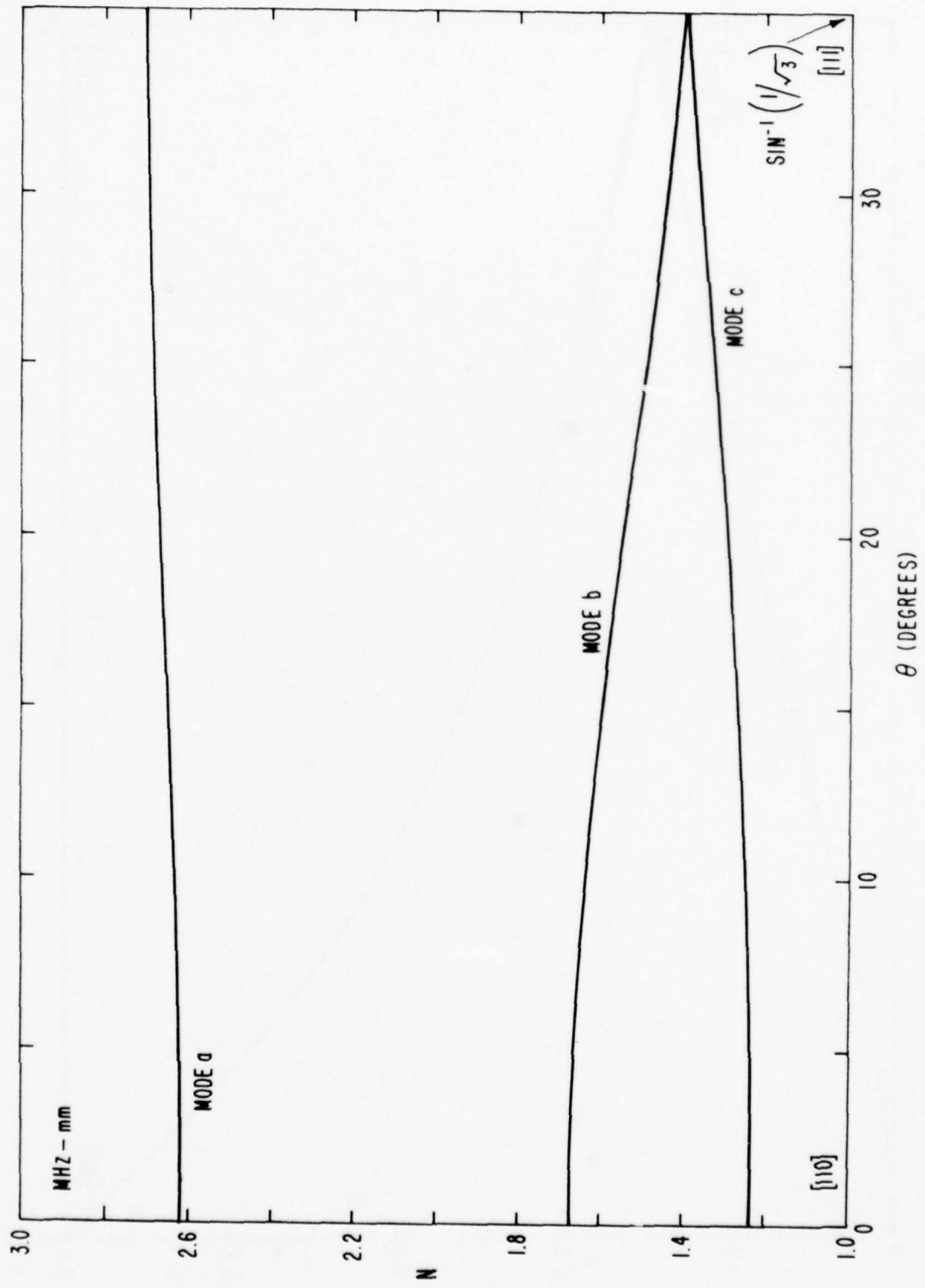


FIGURE 5. FREQUENCY CONSTANTS FOR  $(YXW\ell)45^\circ/\theta$  CUTS OF GALLIUM ARSENIDE.

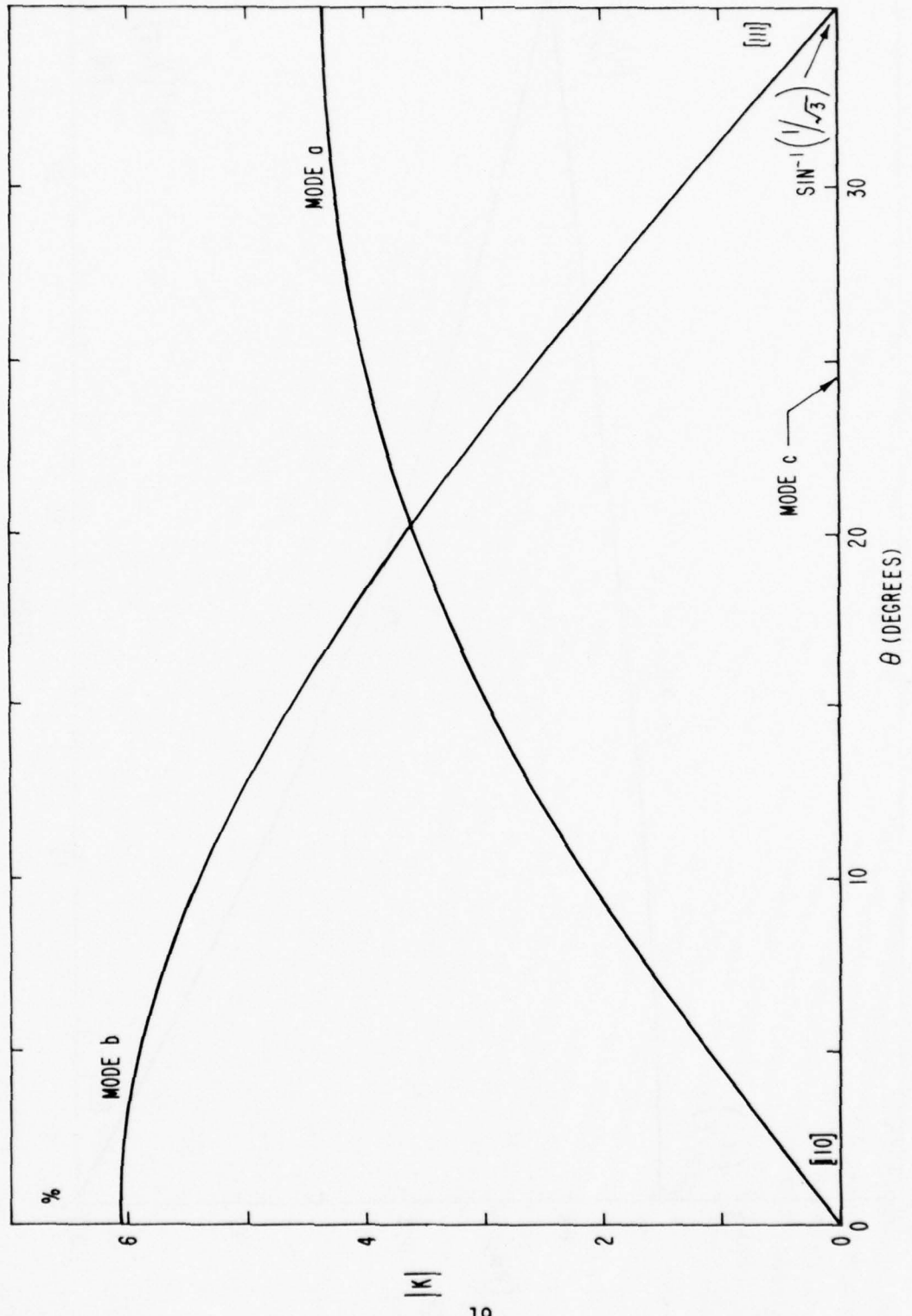


FIGURE 6. PIEZOELECTRIC COUPLING FACTORS OF  $(YXW\theta)45^\circ/\theta$  CUTS OF GALLIUM ARSENIIDE.

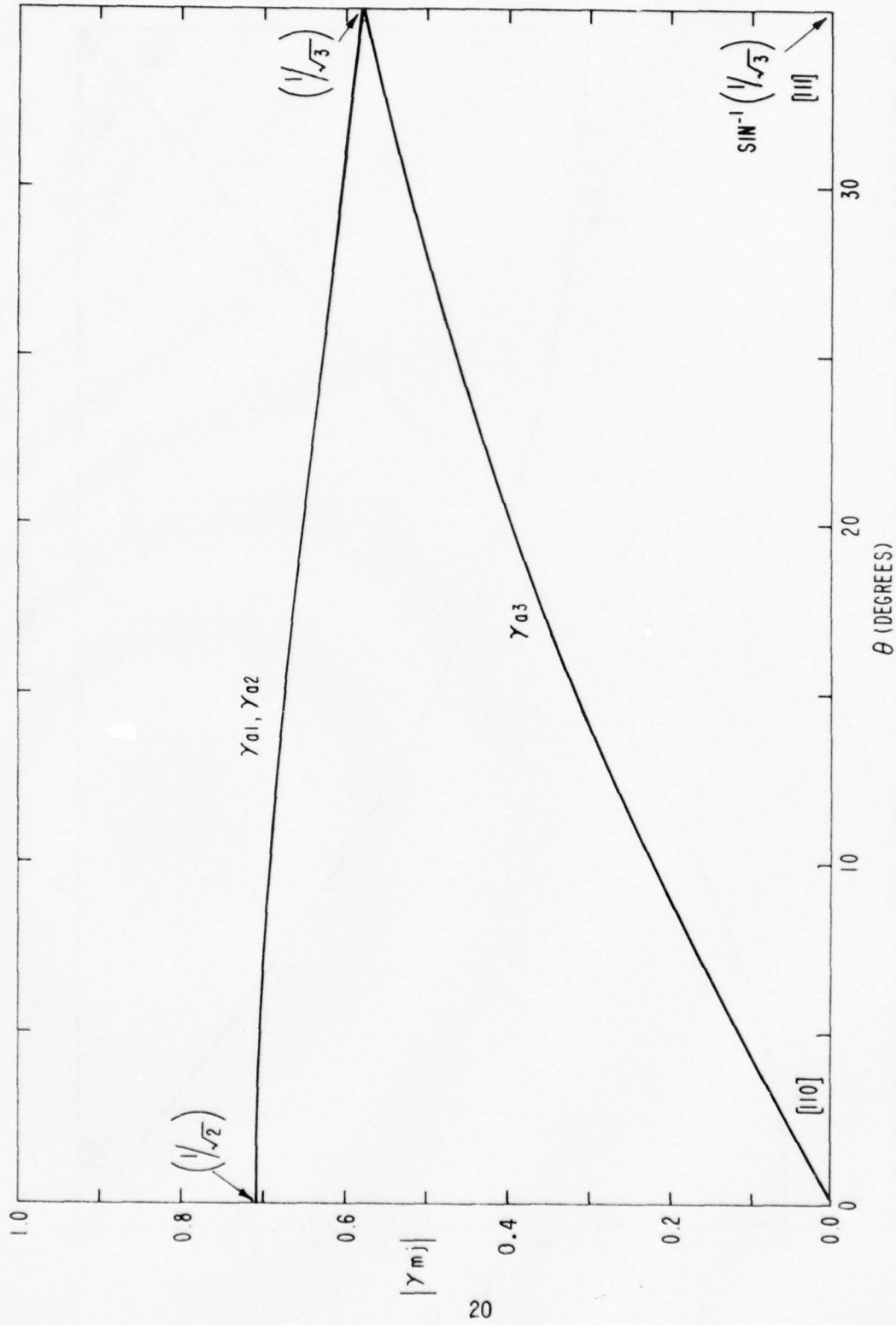


FIGURE 7. DIRECTION COSINES OF PARTICLE MOTION FOR  $(YXwz)45^\circ / \theta$  CUTS OF GALLIUM ARSENIIDE: MODE a.

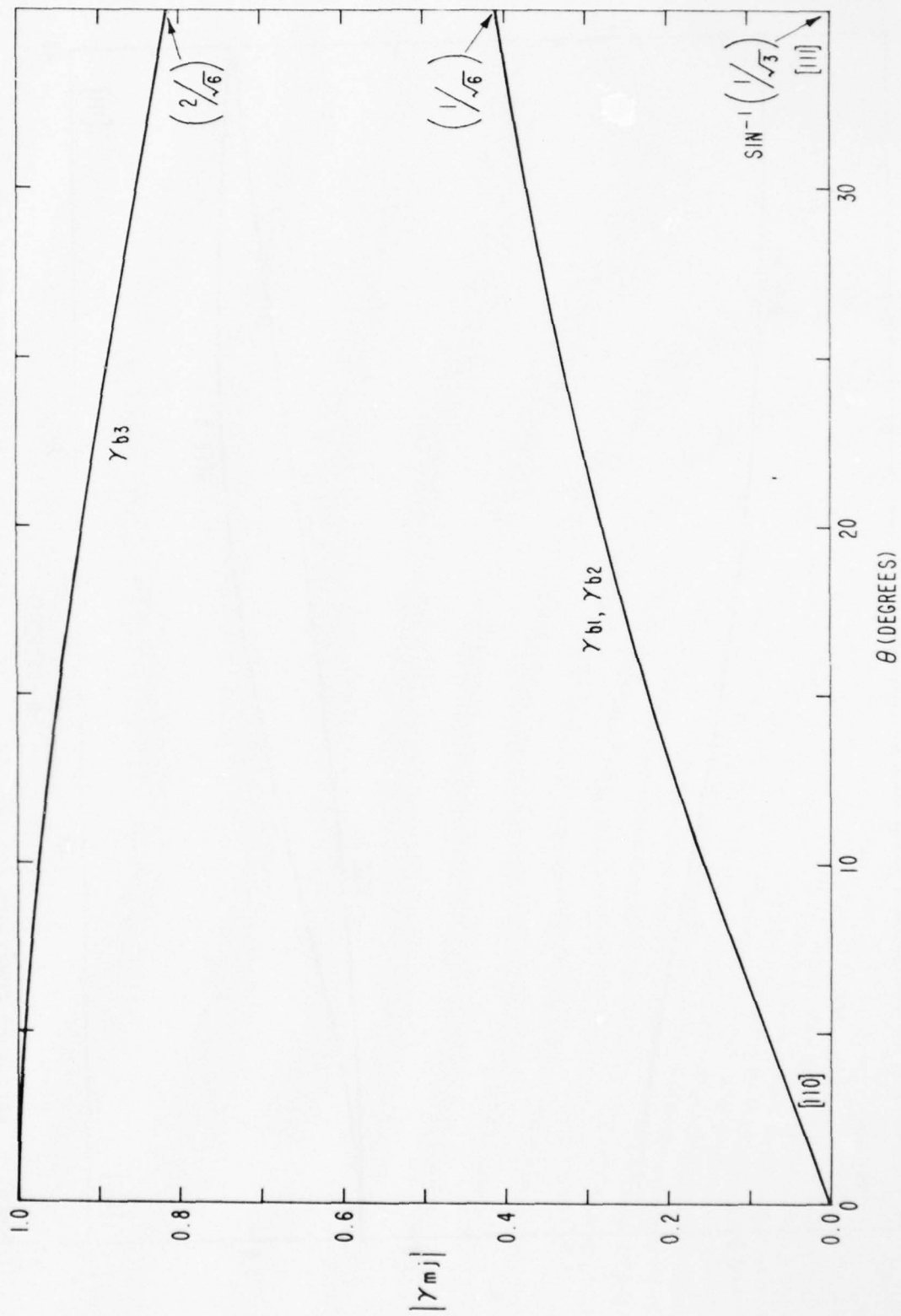


FIGURE 8. DIRECTION COSINES OF PARTICLE MOTION FOR  $(YX_{WZ})45^\circ/\theta$  CUTS OF GALLIUM ARSENIIDE: MODE b.

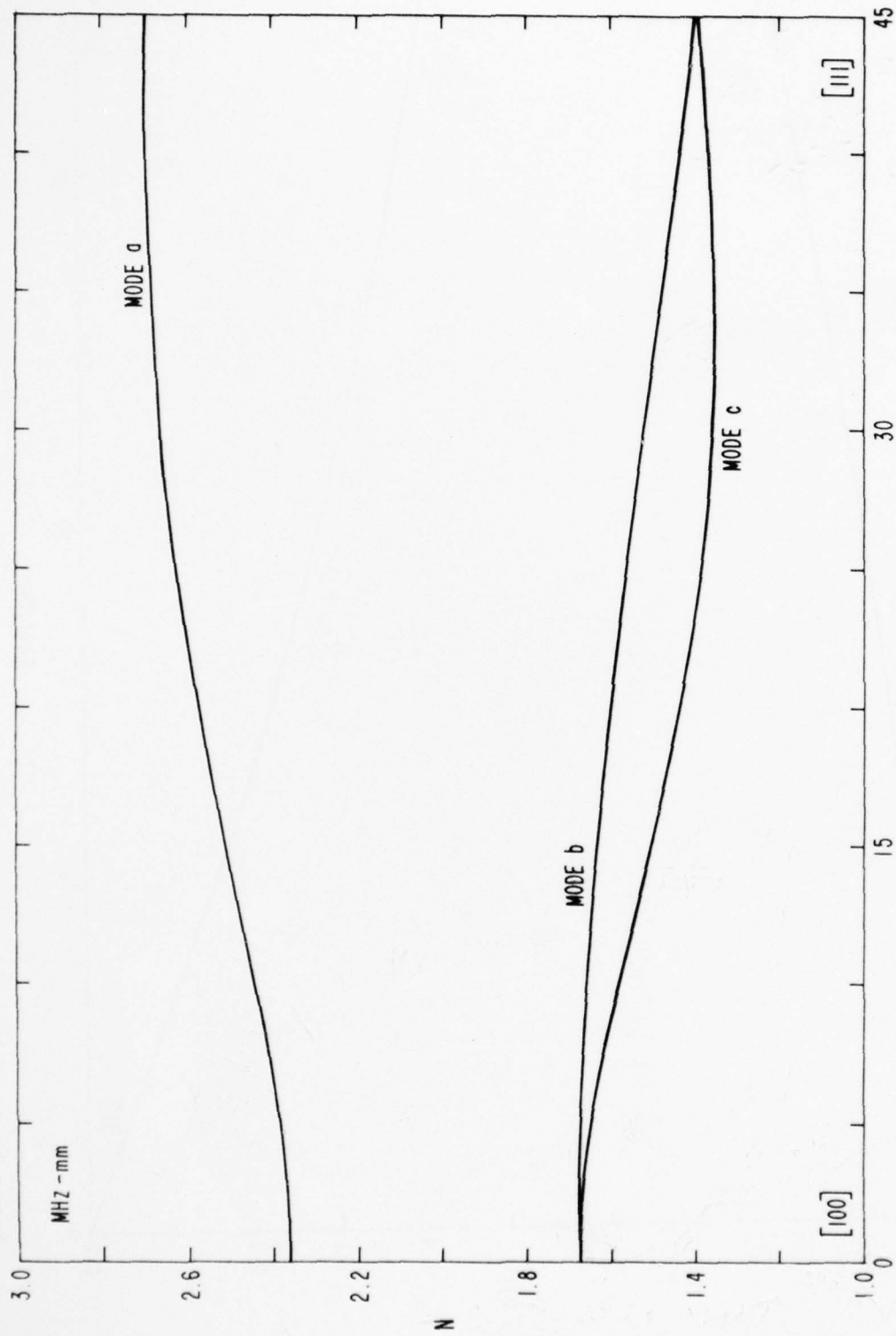


FIGURE 9. FREQUENCY CONSTANTS FOR  $(YXw\phi)_\phi/\tan^{-1}(\sin \phi)$  CUTS OF GALLIUM ARSENIIDE.

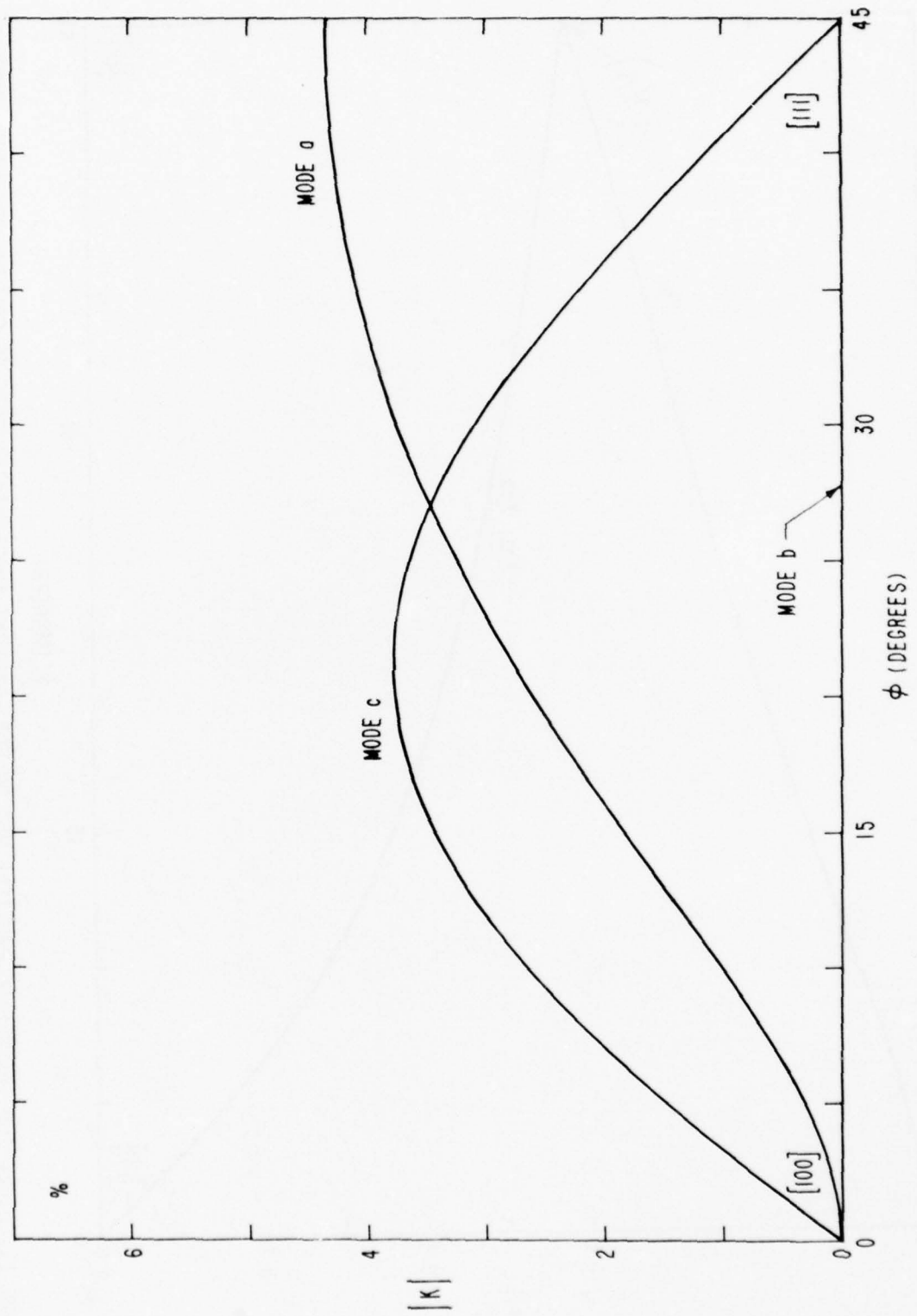


FIGURE 10. PIEZOELECTRIC COUPLING FACTORS OF  $(YXw\epsilon)_\phi / \tan^{-1}(\sin \phi)$  CUTS OF GALLIUM ARSENIDE.

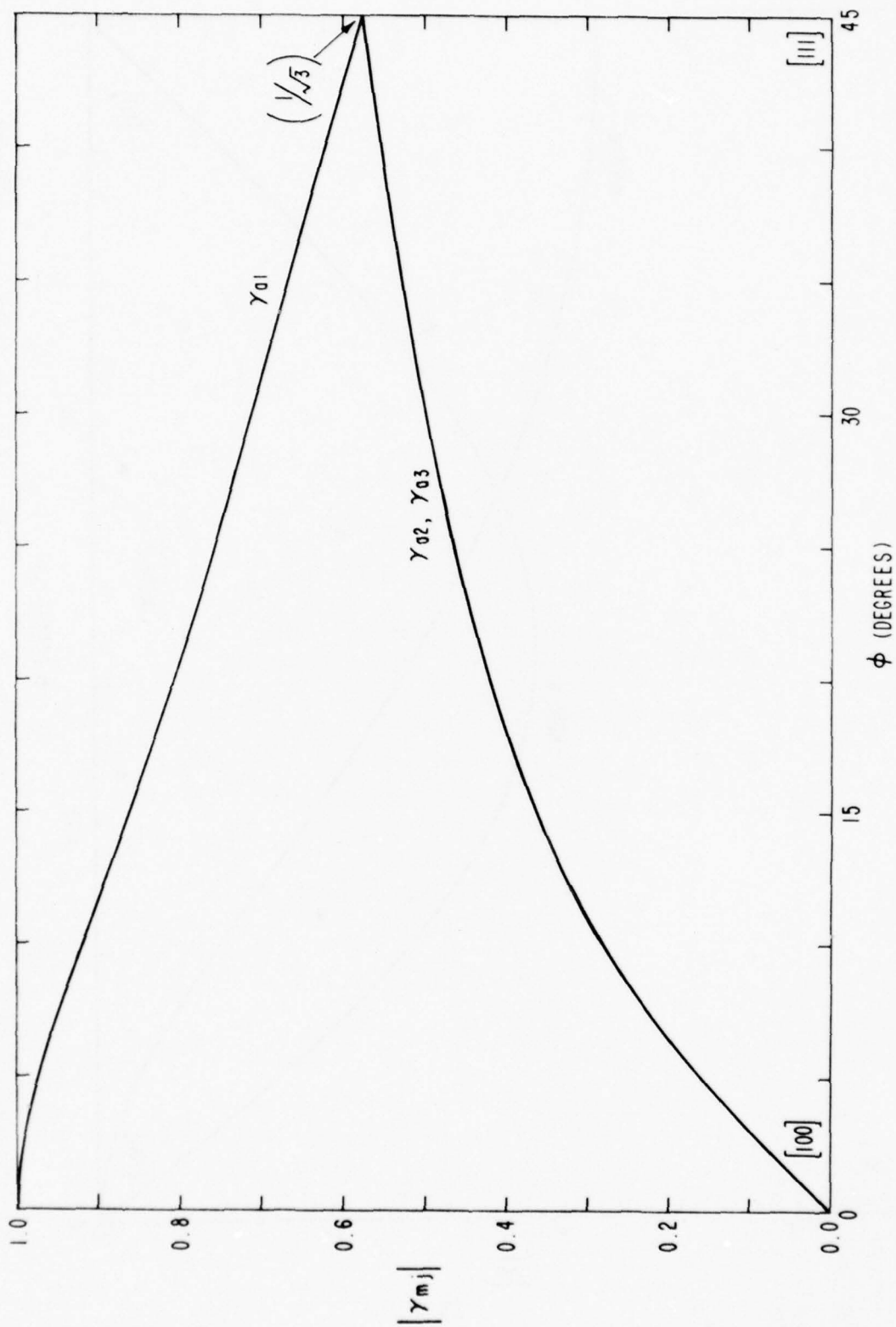


FIGURE 11. DIRECTION COSINES OF PARTICLE MOTION FOR  $(YXwz)_\phi / \tan^{-1}(\sin \phi)$  CUTS OF GALLIUM ARSENIIDE: MODE a.

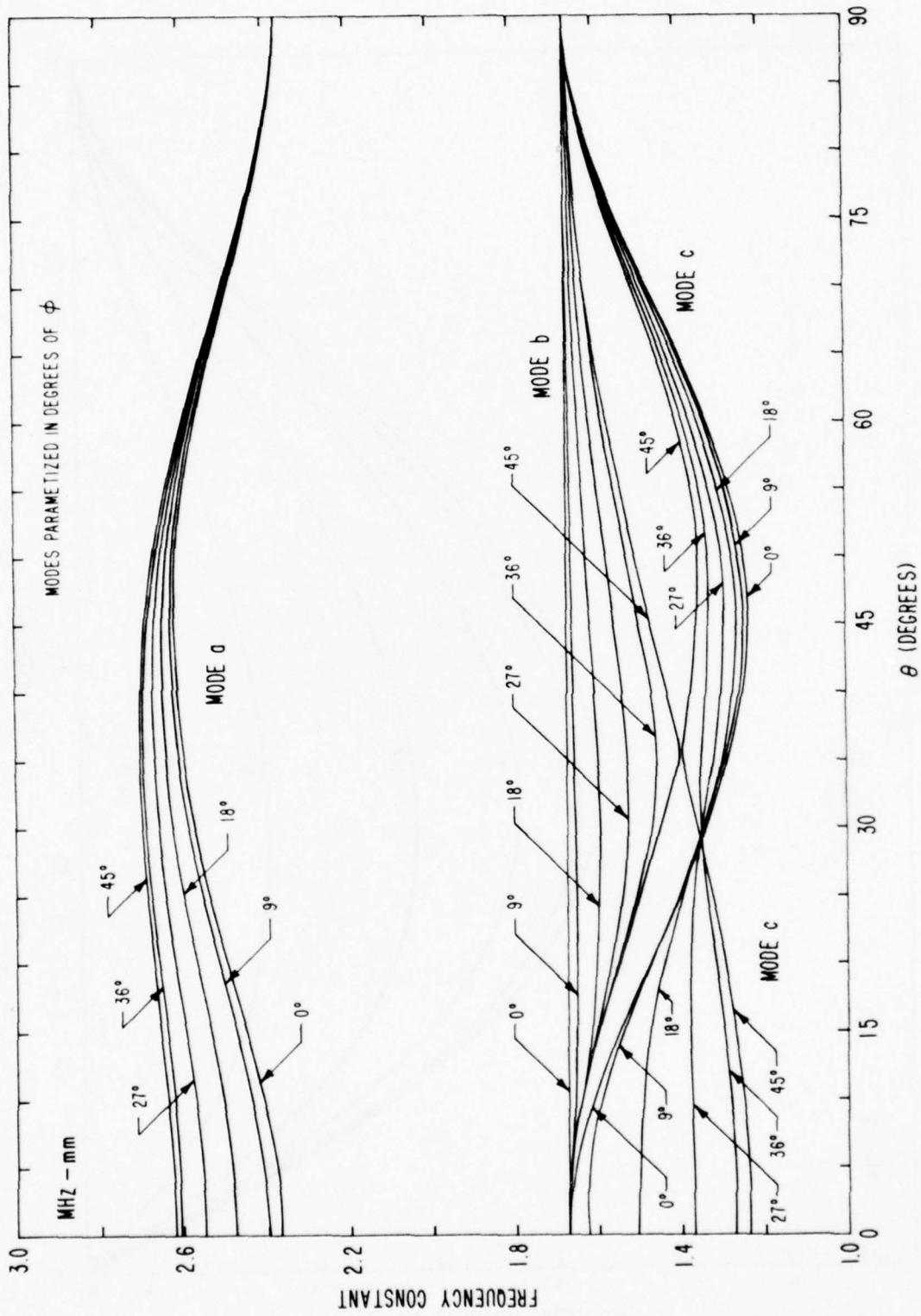


FIGURE 12. FREQUENCY CONSTANTS OF DOUBLY ROTATED CUTS OF GALLIUM ARSENIDE.

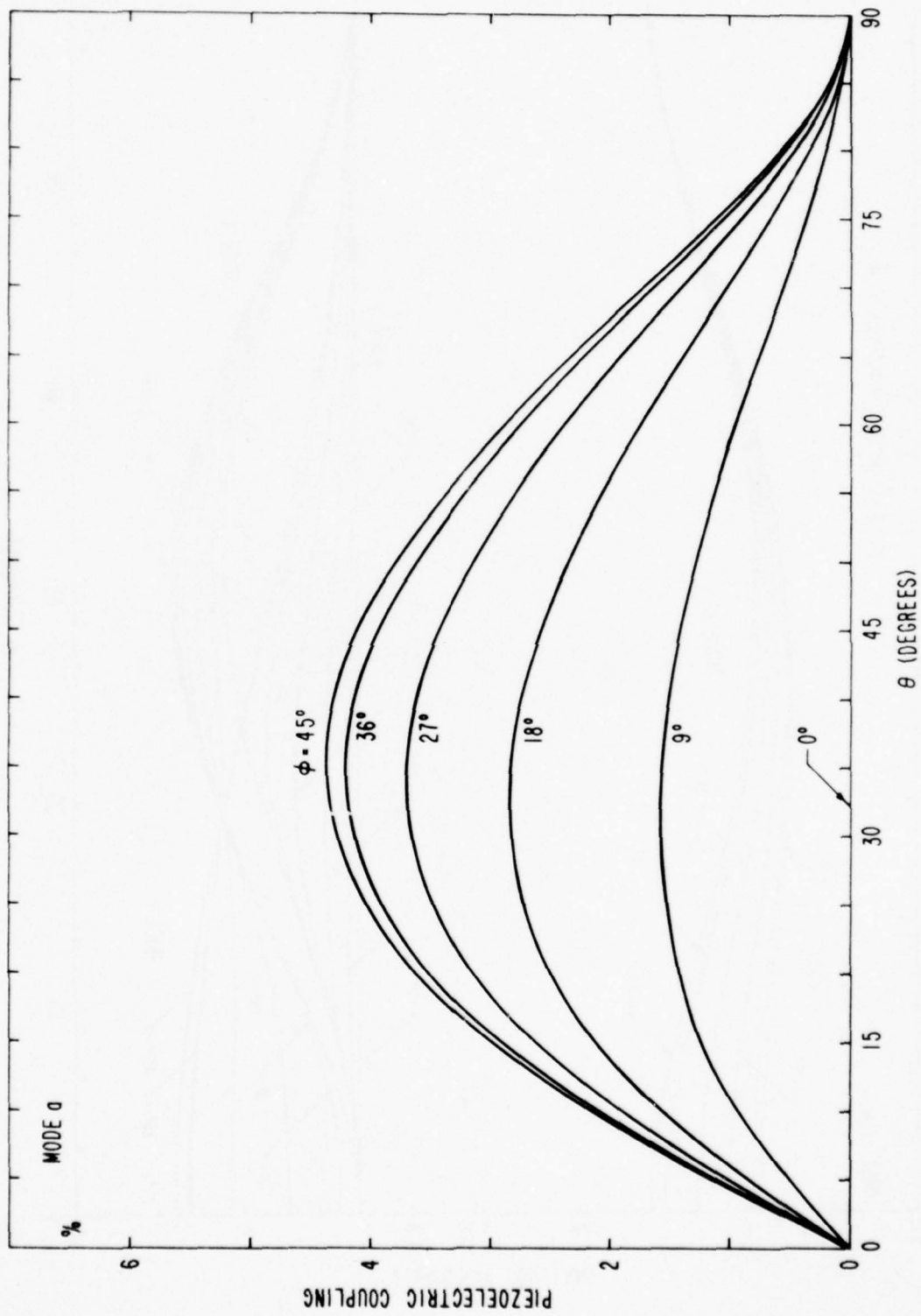


FIGURE 13. PIEZOELECTRIC COUPLING FACTORS OF DOUBLY ROTATED CUTS OF GALLIUM ARSENIDE: MODE a.

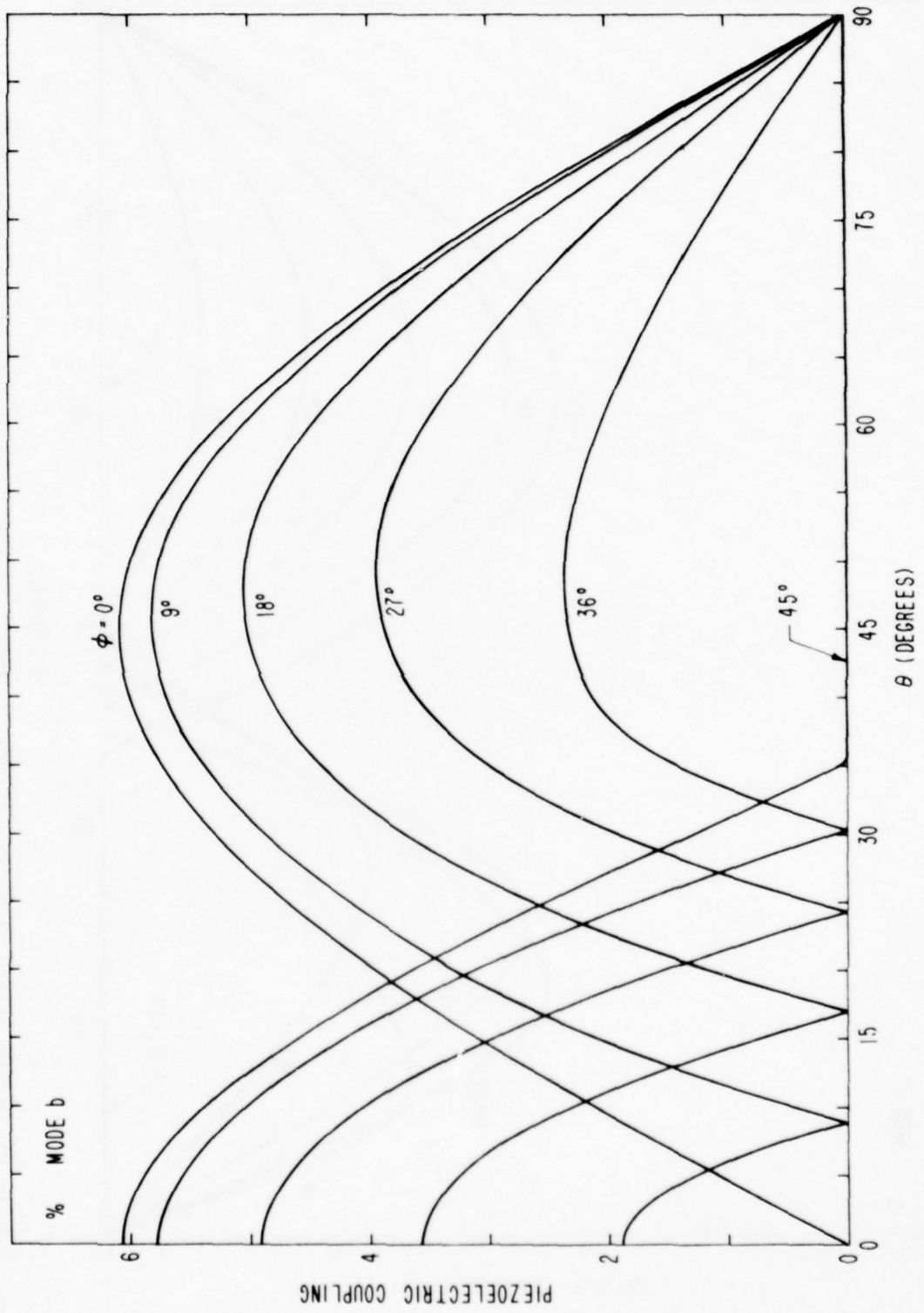


FIGURE 14. PIEZOELECTRIC COUPLING FACTORS OF DOUBLY ROTATED CUTS OF GALLIUM ARSENIIDE: MODE b.

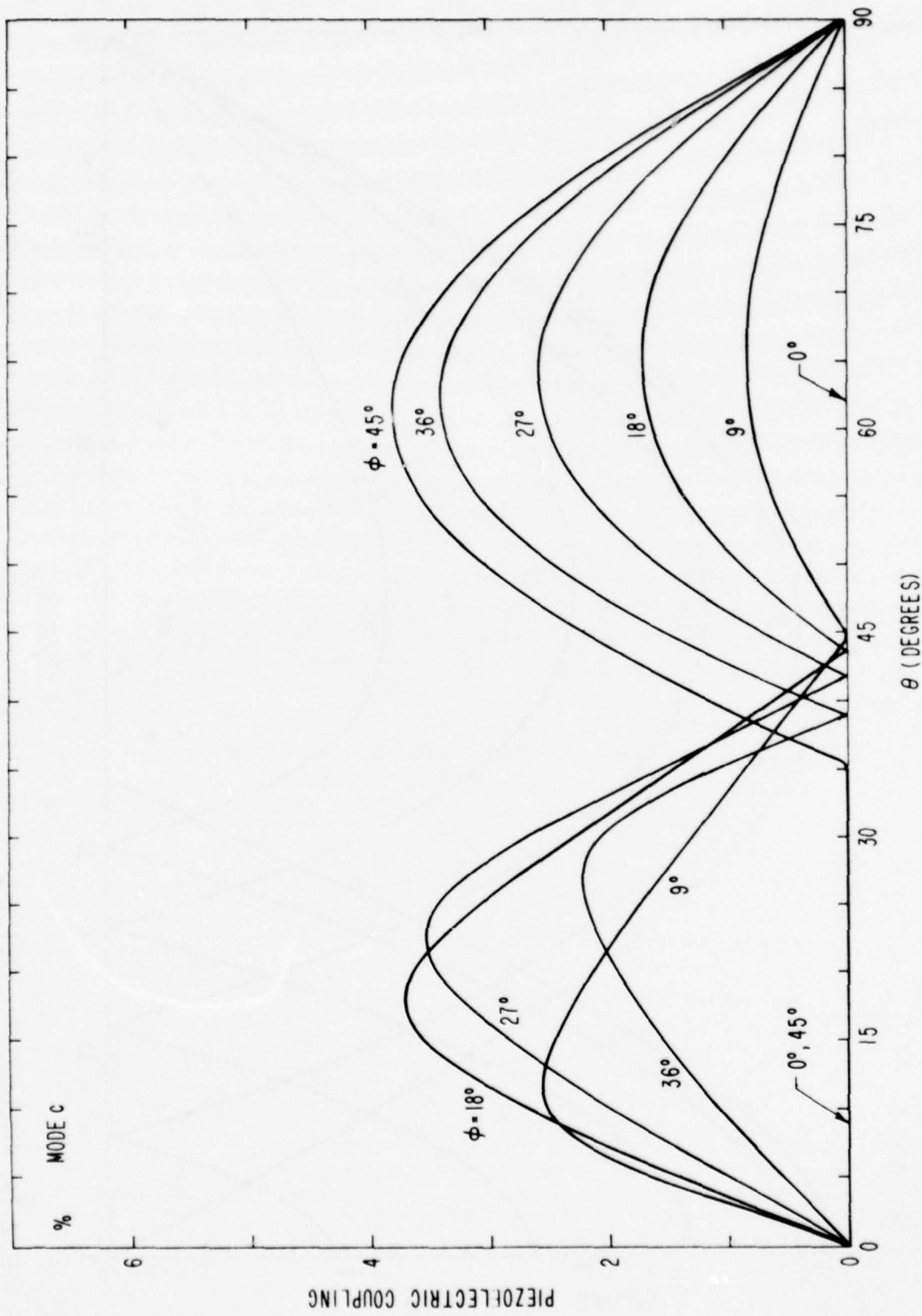


FIGURE 15. PIEZOELECTRIC COUPLING FACTORS OF DOUBLY ROTATED CUTS OF GALLIUM ARSENIDE: MODE C.

## VIBRATIONS OF DOUBLY ROTATED CUBIC CRYSTAL PLATES

The simple thickness vibrations of a crystal plate are those that do not depend upon lateral coordinates. Lateral variations make the problem much more complicated<sup>45</sup>. Taking the plate thickness direction to coincide with the wave propagation direction discussed in the previous section, the solution to the plate vibration problem is obtained by applying the appropriate boundary conditions at the plate surfaces. This was first done consistently by Tiersten<sup>46,47</sup> for traction-free surfaces and an insulating crystal. Because of the piezoelectric effect, all three thickness modes are coupled at the boundaries in the general case of complete anisotropy. Mass-loading was considered by Yamada and Niizeki<sup>48</sup>, who derived the input admittance of the plate vibrator as

$$Y_{\text{input}} = j\omega C_0 / \left[ 1 - \sum_m^3 k_m^2 \tan x_m / x_m \right], \quad (16)$$

where

$$C_0 = \epsilon A / 2h, \quad (17)$$

$$x_m = \omega h / \sigma_m, \quad (18)$$

and  $k_m$  is obtained from Equation (15).  $C_0$  is the static capacitance,  $A$  is the area of the plate portion under consideration, and  $2h$  is the plate thickness. Conditions under which a single mode may be considered by itself are discussed in Reference 6; since these conditions are nearly always fulfilled for the materials in Table 6, we consider a single mode in the sequel. When the conditions are not fulfilled, the treatment of Reference 6 must be followed.

As discussed in the last section, if the crystal is not insulating, but semiconducting, the dielectric permittivity will become complex. From the fact that the piezo-stiffening term then becomes complex,  $\bar{\epsilon}_m$  becomes complex as well, so, from Equations (5), (15), (17) and (18), the various factors in Equation (16) for the input admittance of the crystal vibrator are complex.

Explicit expressions for various quantities of interest are given in Table 9, neglecting carrier diffusion, where Equation (4) can be written; the effect of inclusion of the diffusion term is given in Reference 4.

Viscous loss is accounted for by adding to the elastic stiffnesses a term  $j\omega\eta_m$ , where  $\eta_m$  is a modal viscosity. This has an effect similar to the introduction of the imaginary permittivity term, but the frequency variation is different. One distinguishes between the acoustic time constant

$$\tau_m = \eta_m / \bar{\epsilon}_m, \quad (19)$$

and the electrical time constant

$$\tau = \epsilon / \sigma \quad (20)$$

TABLE 9. PHYSICAL PARAMETERS FOR INSULATING AND SEMICONDUCTING CRYSTALS.

Quantity	Unit	Insulator		Semiconductor	
		Symbol	Relation	Symbol	Relation
Dielectric Permittivity	F/m	$\epsilon$	$\epsilon$	$\epsilon^*$	$\frac{\epsilon(1+j\omega\tau)}{(j\omega\tau)}$
Elastic Stiffness	Pa	$\bar{c}$	$c + e^2/\epsilon$	$\bar{c}^*$	$\bar{c} \cdot F$
Acoustic Velocity	m/s	$v$	$\sqrt{\bar{c}/\rho}$	$v^*$	$v \cdot F^{1/2}$
Piezoelectric Constant	C/m <sup>2</sup>	$e$	$e$	$e^*$	$e$
Mass Density	kg/m <sup>3</sup>	$\rho$	$\rho$	$\rho^*$	$\rho$
Time Constant	s	$\tau$		$\tau^*$	$\epsilon / \sigma$
Acoustic Wavenumber	m <sup>-1</sup>	$\kappa$	$\omega/v$	$\kappa^*$	$\kappa \cdot F^{-1/2}$
Piezoelectric Coupling Factor	-	$k$	$ e  / \sqrt{\epsilon \bar{c}}$	$k^*$	$k \cdot F^{-1/2} (j\omega\tau) / (1+j\omega\tau)$

$$F = \{1 - k^2 / (1 + j\omega\tau)\}$$

by the different frequency dependencies of the terms containing these factors. For example, the expression for the effective elastic constant in the presence of both acoustic and electrical conductivity losses is

$$\bar{\epsilon}^* = \bar{\epsilon} \cdot [1 + j(\omega\tau_m + k^2/(\omega\tau))]. \quad (21)$$

When the plate surfaces are coated with a thin layer having a mass  $\bar{m}$  per unit area on each surface, then, providing that the coating is small enough to neglect acoustic transit times through it, the effect may be expressed in its influence on  $Y_{input}$  as follows:

$$Y_{input} = j\omega C_0 / \left\{ 1 - \sum_m^3 \left[ \left( \frac{k_m^2}{1 - \bar{\mu} x_m \tan x_m} \right) \cdot \frac{\tan x_m}{x_m} \right] \right\}. \quad (22)$$

In Equation (22), the quantity  $\bar{\mu}$  is the reduced mass loading:

$$\bar{\mu} = \bar{m} / \rho h. \quad (23)$$

The relation (22) holds also when the terms become complex; this fact will be exploited in the sequel. An air gap may be used to excite the resonators, rather than having electrodes deposited directly on the plates. In this case the effect is easily taken into account by dividing  $C_0$  and the  $k_m^2$  in Equations (16) and (22) by the factor  $(1 + C_0/C_L)$ , where  $C_L$  is the air gap capacitance (or value of a discrete capacitor placed in series with the crystal).

#### EQUIVALENT NETWORK FOR SEMICONDUCTING PIEZOELECTRIC PLATES

From the input admittance given in the last section the equivalent electrical network can be synthesized. This will be briefly sketched here for a single mode, although the network can be extended to two or three modes<sup>6</sup>. Starting from Equation (16), written for a single mode, the admittance of a shunt capacitance  $C_0$  is subtracted out, leaving

$$j\omega C_0 (k^2 T) / (1 - k^2 T). \quad (24)$$

Further subtraction of a negative series  $C_0$  leave the admittance

$$j\omega C_0 k^2 T \quad (25)$$

In Equations (24) and (25)  $T$  equals  $\tan x/x$ . The admittance of Equation (25) is realized as a transformer shunting a transmission line, the transformer representing the piezoelectric transduction mechanism, and the line representing the mechanical vibrations. The transformer turns ratio is

$$n = e_m A / 2h \quad (26)$$

and the transmission line admittance is

$$Y_0 = 1 / A \rho v_m . \quad (27)$$

When the conductance is not zero, the network appears as shown in Figure 16. Here the capacitances  $C_0$  are shunted by conductances  $G_0$ , where

$$G_0 = \sigma A / 2h , \quad (28)$$

and  $\sigma$  is the sample conductivity (reciprocal resistivity). When diffusion effects are considered one will have an effective, frequency-dependent, value of  $\sigma$  instead. In Figure 16,  $Y_0$  and  $x$  will also be complex as discussed above. The values for these are given in Table 10.

Mass loading effects are taken into account in the network of Figure 16 by simply adding in series with the transmission line, at the end where the piezoelectric transformer is located, an inductance  $L$ , where

$$L = \bar{m} A . \quad (29)$$

This relation follows from performing a network synthesis on Equation (22).

The effect of large viscous loss on the behavior of the equivalent circuit of a vibrator with zero conductivity is shown in Figures 17 and 18. In Figure 17 is shown the impedance circle representation;  $Z_{in} = 1/Y_{input}$ . Figure 18 shows the real and imaginary parts of the input impedance as function of frequency normalized to the frequency where the lossless transmission line would be one quarter wavelength long.

Measurement methods pertaining to low- $Q$  vibrators are discussed in References 49-54. With the inclusion of conductivity terms the general appearances of Figures 17 and 18 will remain as shown, but the expressions for the real and imaginary parts of the impedance or admittance will be more complicated.

#### NONDESTRUCTIVE EVALUATION OF OXIDE LAYER MASS

The properties and performance of planar integrated circuit devices<sup>55</sup> depend on the production of inert dielectric oxide layers on semiconductors. A gate oxide layer may typically be 1000 Å, whereas an isolation oxide for passivation is perhaps a micrometer thick. It is of technological interest to have a simple and rapid nondestructive test of the amount of material added to the semiconductor in both cases. For this purpose, use of the crystal as an acoustic resonator enables the critical frequencies associated with the resonance to be measured<sup>56</sup>. Since these may be measured with great accuracy in an air gap holder<sup>57</sup>, and since the frequencies are simply related to the parameters of the equivalent network, the mass loading due to the oxide or passivation layer may be deduced.

In the case of gallium arsenide, some of the various oxide species that can exist are enumerated in Table 11, with their room temperature densities. From the table one can see that the densities are not too far

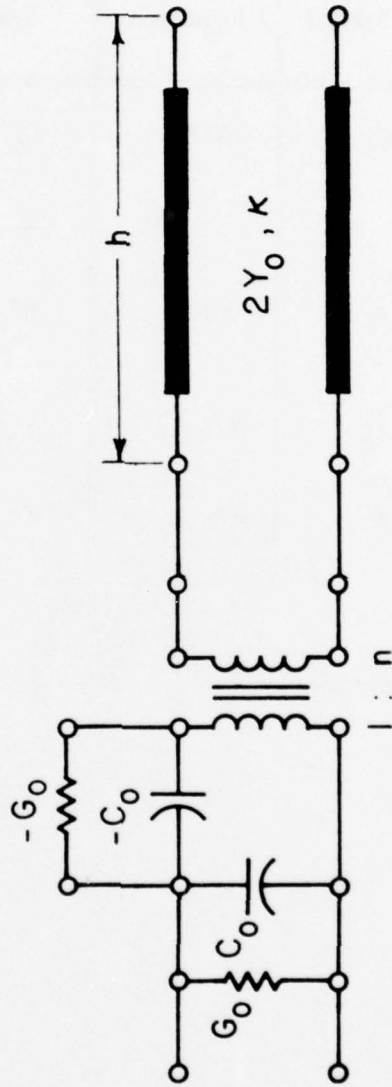


FIGURE 16. EXACT EQUIVALENT NETWORK FOR A SINGLE DRIVEN MODE IN A PIEZOELECTRIC, SEMICONDUCTING CRYSTAL PLATE.

TABLE 10. ELECTRICAL NETWORK PARAMETERS FOR INSULATING AND SEMI-CONDUCTING CRYSTALS.

Quantity	Unit	Insulator		Semiconductor	
		Symbol	Relation	Symbol	Relation
Static Capacitance	F	$C_0$	$\epsilon A/2h$	$C_0^*$	$C_0 + G_0/j\omega$
Static Conductance	S			$G_0$	$\sigma A/2h$
Piezoelectric Transformer Ratio	C/m	$n$	$Ae/2h$	$n^*$	$n$
Acoustic Admittance	s/kg	$Y_0$	$1/A \rho v$	$Y_0^*$	$Y_0 \cdot F^{-1/2}$
Normalized Frequency Variable	-	$X$	$\kappa h$	$X^*$	$X \cdot F^{-1/2}$

$$F = \{1 - k^2 / (1 + j\omega\tau)\}$$

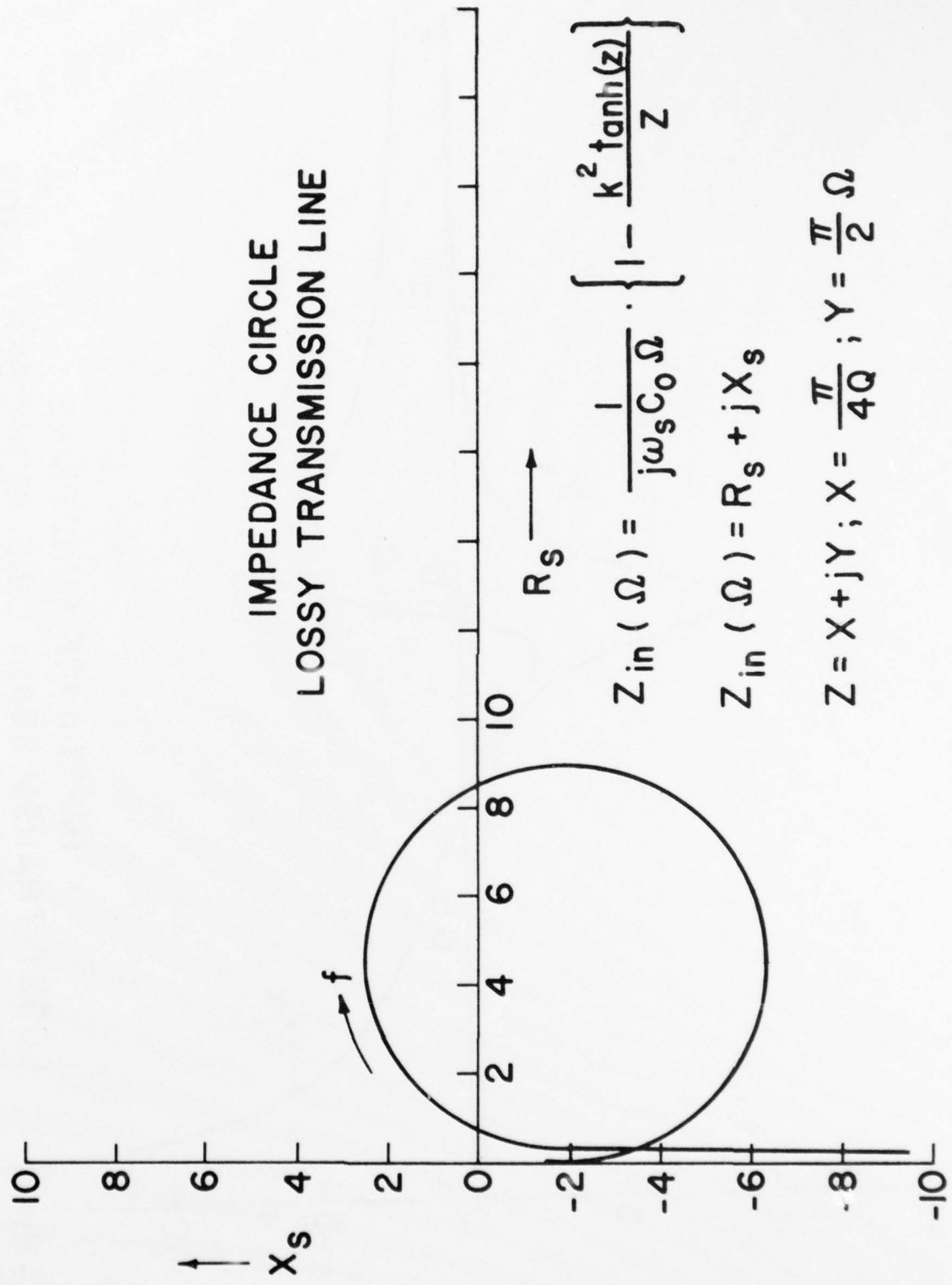
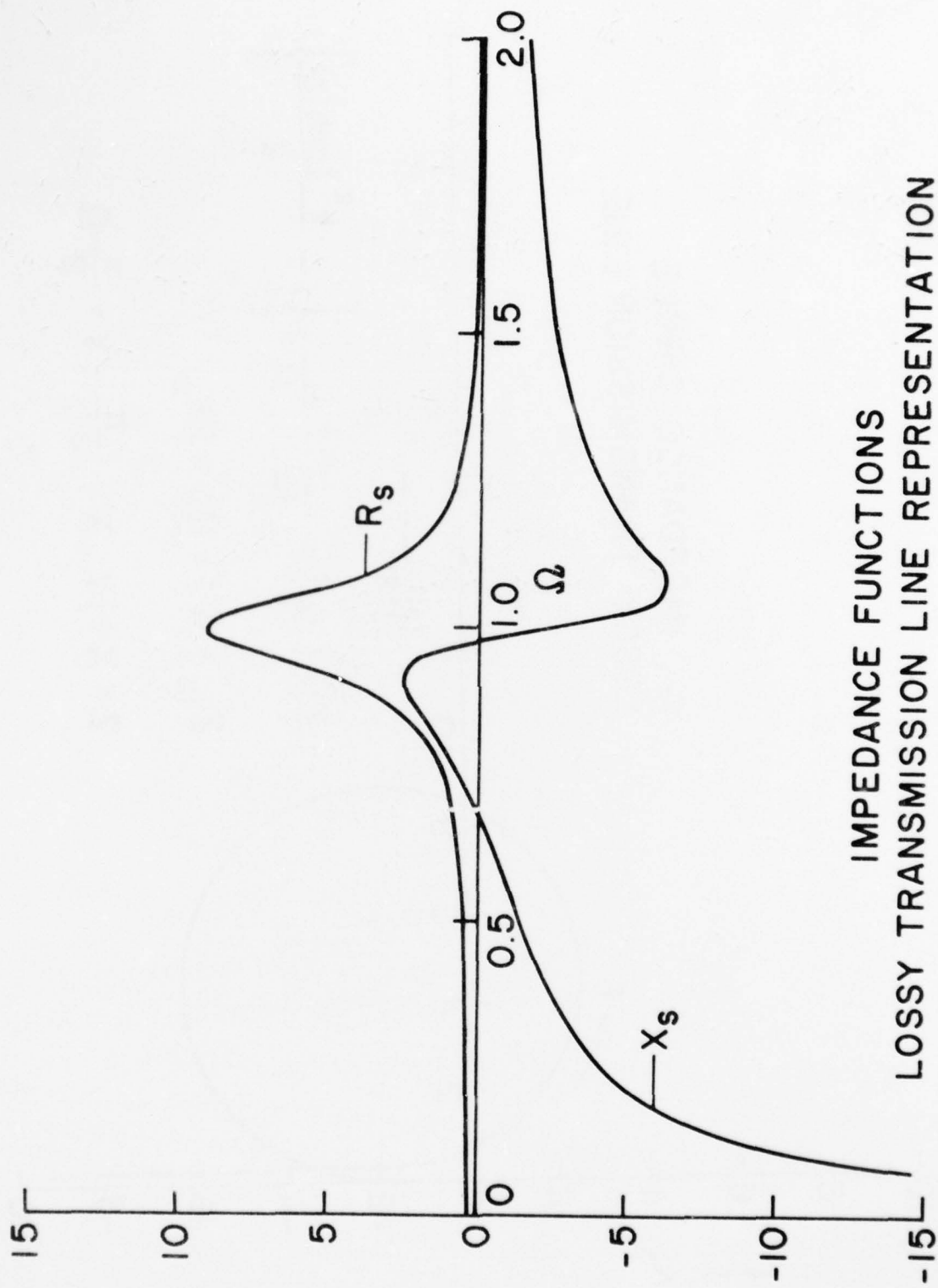


FIGURE 17. IMPEDANCE CIRCLE REPRESENTATION OF LOSSY TRANSMISSION LINE EQUIVALENT NETWORK.



### IMPEDANCE FUNCTIONS LOSSY TRANSMISSION LINE REPRESENTATION

FIGURE 18. REACTANCE AND RESISTANCE VERSUS NORMALIZED FREQUENCY FOR LOSSY TRANSMISSION LINE EQUIVALENT NETWORK.

TABLE 11. ROOM TEMPERATURE DENSITIES OF OXIDES.

Oxide	Density
	$10^3 \text{ kg/m}^3$
$\alpha\text{-Ga}_2\text{O}_3$	6.5
$\beta\text{-Ga}_2\text{O}_3$	5.9
$\delta\text{-Ga}_2\text{O}_3$	5.0
$\text{As}_2\text{O}_3$	3.9
$\text{As}_2\text{O}_5$	4.3
$\text{Ga}_2\text{O}$	4.8
$\text{Ga As O}_4$	4.2

removed from that of GaAs, averaging about  $3 \times 10^3 \text{ kg/m}^3$ . A knowledge of the particular oxide or passivation layer constituent(s) under consideration determines the layer thickness once the added mass is found from the frequency shift.

An example of the procedure involved follows: The sample, in plate form, is measured to determine the approximate thickness. With the sample orientation known, the frequency constants are known, e.g., from plots like those in Figure 12. The corresponding piezoelectric coupling factors  $|k_m|$  are likewise known; the coupling determines how strongly the mode or modes in question can be driven by the measurement apparatus. The frequencies

$$f_m = N_m / (2h) \quad (30)$$

are then calculated; about these frequencies lie the resonance regions. Odd harmonics of  $f_m$  are also piezoelectrically excitable. Once the resonance regions are approximately determined, the sample is placed in an air gap holder, and the gap set to a prescribed value. Then the frequency spectrum is explored by any of several methods<sup>58-63</sup>. Some point on the immittance circle, appropriate to both the measurement instrument and the resonator under test, is selected to characterize the resonator plate. The frequency at this point is recorded. It may be necessary to make the measurement in a modest vacuum for best results, particularly if the mode  $a$  is used. The sample is then removed from the holder and processed for oxide layer growth or passivation layer deposition, etc. After completion of treatment, it is reinserted into the air gap holder and remeasured at the same point on the immittance circle as before (for example, both measurements could be made at the condition of resonance, where the imaginary part of the immittance is zero and the real part is small; or it could be made at the frequency of maximum resistance, or of minimum impedance, etc.).

The shift of the chosen critical frequency point with sample treatment is a very sensitive measure of  $\bar{\mu}$ , and forms the basis for the quartz micro-balance<sup>64-68</sup>. In the present instance the frequency shift could be correlated with  $\bar{\mu}$  by means of the equivalent circuit of Figure 16, augmented as described by the addition of a lumped inductor. The circuit describes the immittance versus frequency of the vibrator, and the effect of the air gap is incorporated, as discussed, by modification to  $k_m$  and  $C_0$ .

Frequency measurements are among the most accurate measurements that can be made, and accuracies of fractions of a part per million are commonplace. To get an appreciation for the sensitivity of the method, consider a plate having a thickness of 1 mm. If the frequency changes by  $1 \times 10^{-6}$  on a normalized basis, and if this frequency change was due solely to a change in resonator thickness, then the thickness change would be 1 mm times  $1 \times 10^{-6}$ , or  $1 \mu\text{m}$ . Since a fractional frequency deviation of  $1 \times 10^{-7}$  ought to be readily discernable with present-day measurement equipment, and since the plate thicknesses are apt to be only fractions of a millimeter, the method is potentially capable of measuring very small mass changes. The method does depend, however, on the accuracy with which frequency can be repeatably measured, and this depends on a number of things. Perhaps chief among these, aside from physical reproducibility, as in maintaining the air gap value, is

temperature variation. For quartz, with its zero temperature coefficient cuts, the situation is eased. Other materials lack such cuts, and this includes the majority of crystals. Approximate values for the temperature coefficients of the elastic stiffnesses of gallium arsenide, calculated from data in Reference 22, are given in Table 7. Assuming a (111) cut, the first order temperature coefficient of frequency for the a mode is approximately  $-72 \times 10^{-6}/K$ ; the value for a (110) cut (b mode) is  $-34 \times 10^{-6}/K$ . One sees from these numbers that a high stability oven is required for measurements in the  $10^{-6}$  range for gallium arsenide if monolayer masses are to be measured. A very modest oven, however, permits one to measure equivalent thickness changes in the 100 to 1000 Å range, and beyond. This is just the regime encountered in integrated circuit electronics.

#### CONCLUSIONS

Acoustic wave propagation in cubic crystals has been considered from the standpoint of establishing the properties germane to the use of such crystals as piezoelectric plate vibrators. An equivalent electrical network was developed for piezoelectric semiconducting plate vibrators, including the presence of lumped masses on the plate surfaces. The frequency change due to the added surface mass was shown to be a very sensitive indicator of the quantity of mass added, and can serve to monitor the surface layer. Calculations were carried out for gallium arsenide doubly rotated plates; these included acoustic velocities and piezoelectric coupling factors for the three thickness modes.

## REFERENCES

1. A. R. Hutson, J. H. McFee, and D. L. White, "Ultrasonic Amplification in CdS," *Phys. Rev. Lett.*, Vol. 7, 15 September 1961, pp. 237-239.
2. K. Blötekjaer and C. F. Quate, "The Coupled Modes of Acoustic Waves and Drifting Carriers in Piezoelectric Crystals," *Proc. IEEE*, Vol. 52 April 1964, pp. 360-377.
3. J. J. Kyame, "Conductivity and Viscosity Effects on Wave Propagation in Piezoelectric Crystals," *J. Acoust. Soc. Amer.*, Vol. 26, November 1954, pp. 990-993.
4. A. R. Hutson and D. L. White, "Elastic Wave Propagation in Piezoelectric Semiconductors," *J. Appl. Phys.*, Vol. 33, January 1962, pp. 40-47.
5. G. Arlt, "Resonance-Antiresonance of Conducting Piezoelectric Resonators," *J. Acoust. Soc. Amer.* Vol. 37, January 1965, pp. 151-157.
6. A. Ballato, "Doubly Rotated Thickness Mode Plate Vibrators," in *Physical Acoustics: Principles and Methods*, (W. P. Mason and R. N. Thurston, eds.), Vol. 13, Chap. 5. Academic Press, New York, 1977, pp. 115-181.
7. *IEEE Standard on Piezoelectricity*, Std 176-1978, The Institute of Electrical and Electronics Engineers, Inc., 345 East 47th Street, New York, NY 10017.
8. J. Lamb and J. Richter, "Anisotropic Acoustic Attenuation with New Measurements for Quartz at Room Temperatures," *Proc. Roy. Soc. (London)*, Vol. A293, 1966, pp. 479-492.
9. R. M. White, "Surface Elastic Waves," *Proc IEEE*, Vol. 58, August 1970 pp. 1238-1276.
10. K. H. Yen, K. L. Wang, and R. S. Kagiwada, "Efficient Bulk Wave Excitation on ST Quartz," *Electron. Lett.*, Vol. 13, January 1977, pp. 37-38.
11. J. F. Nye, *Physical Properties of Crystals: their representation by tensors and matrices*. (Clarendon Press, Oxford, 1957).
12. R. F. S. Hearmon, *An Introduction to Applied Anisotropic Elasticity*. London: Oxford, 1961.

13. D. I. Bolef and M. Menes, "Elastic Constants of Single-Crystal Aluminum Antimonide," *J. Appl. Phys.* Vol. 31, August 1960, pp. 1426-1427.
14. H. J. McSkimin and D. G. Thomas, "Elastic Moduli of Cadmium Telluride," *J. Appl. Phys.*, Vol. 33, January 1962, pp. 56-59.
15. H. J. McSkimin, A. Jayaraman, P. Andreatch, Jr., and T. B. Bateman, "Elastic Moduli of Gallium Antimonide under Pressure and the Evaluation of Compression to 80 kBar," *J. Appl. Phys.*, Vol. 39, August 1968, pp. 4127-4128.
16. H. J. McSkimin, A. Jayaraman, and P. Andreatch, Jr., "Elastic Moduli of GaAs at Moderate Pressures and the Evaluation of Compression to 250 kBar," *J. Appl. Phys.*, Vol. 38, April 1967, pp. 2362-2364.
17. R. Weil and W. O. Groves, "The Elastic Constants of Gallium Phosphide," *J. Appl. Phys.*, Vol. 39, August 1968, pp. 4049-4051.
18. J. R. Drabble and A. J. Brammer, "The Third-Order Elastic Constants of Indium Antimonide," *Proc. Phys. Soc. (London)*, Vol. 91, March 1967, pp. 959-964.
19. D. Gerlich, "Elastic Constants of Single-Crystal Indium Arsenide," *J. Appl. Phys.*, Vol. 34, September 1963, p. 2915.
20. D. Berlincourt, H. Jaffee, and L. R. Shiozawa, "Electroelastic Properties of the Sulfides, Selenides, and Tellurides of Zinc and Cadmium," *Phys. Rev.*, Vol. 129, February 1963, pp. 1009-1017.
21. F. S. Hickernell and W. R. Gayton, "Elastic Constants of Single-Crystal Indium Phosphide," *J. Appl. Phys.*, Vol. 37, January 1966, p. 462.
22. C. W. Garland and K. C. Park, "Low-Temperature Elastic Constants of Gallium Arsenide," *J. Appl. Phys.*, Vol. 33, February 1962, pp. 759-760.
23. G. Arlt and P. Quadflieg, "Piezoelectricity in III - V Compounds with a Phenomenological Analysis of the Piezoelectric Effect," *Phys. Stat. Sol.*, Vol. 25, January-February 1968, pp. 323-330.
24. K. S. Champlin and G. H. Glover, "Temperature Dependence of the Microwave Dielectric Constant of the GaAs Lattice," *Appl. Phys. Lett.*, Vol. 12, April 1968, pp. 231-232.
25. E. D. Pierron, D. L. Parker, and J. B. McNeely, "Coefficient of Expansion of Gallium Arsenide from -62 to 200 C," *Acta Cryst.*, Vol. 21, August 1966, p. 290.

26. H.J. McSkimin and P. Andreatch, Jr., "Third-Order Elastic Moduli of Gallium Arsenide", *J. Appl. Phys.*, Vol. 38, 1967, pp. 2610-2611.
27. F. E. Borgnis, "Specific Directions of Longitudinal Wave Propagation in Anisotropic Media," *Phys. Rev.*, Vol. 98, May 1955, pp. 1000-1005.
28. M. J. P. Musgrave, "On the Propagation of Elastic Waves in Aelotropic Media. I. General Principles," *Proc. Roy. Soc. (London)*, Vol. A226, 1954, pp. 339-355.
29. M. J. P. Musgrave, "On the Propagation of Elastic Waves in Aelotropic Media. II. Media of Hexagonal Symmetry," *Proc. Roy. Soc. (London)*, Vol. A226, 1954, pp. 356-366.
30. G. F. Miller and M. J. P. Musgrave, "On the Propagation of Elastic Waves in Aelotropic Media. III. Media of Cubic Symmetry," *Proc. Roy. Soc. (London)*, Vol. A236, 1956, pp. 352-383.
31. M. J. P. Musgrave, "The Propagation of Elastic Waves in Crystals and other Anisotropic Media," in Reports on Progress in Physics, (Physical Society, London, 1959), Vol. 22, pp. 74-96.
32. M. J. P. Musgrave, "Elastic Waves in Anisotropic Media," in Progress in Solid Mechanics, I. N. Sneddon and R. Hill, Eds., (Interscience New York, 1961), Vol. II, Chap. II, pp. 61-85.
33. M. J. P. Musgrave, Crystal Acoustics: Introduction to the study of elastic waves and vibrations in crystals, (Holden-Day, San Francisco, 1970).
34. J. deKlerk and M. J. P. Musgrave, "Internal Conical Refraction of Transverse Elastic Waves in a Cubic Crystal," *Proc. Phys. Soc.*, Vol. B68, 1955, pp. 81-88.
35. P. C. Waterman and L. J. Teutonico, "Ultrasonic Double Refraction in Single Crystals," *J. Appl. Phys.*, Vol. 28, February 1957, pp. 266-270.
36. P. C. Waterman, "Orientation Dependence of Elastic Waves in Single Crystals," *Phys. Rev.*, Vol. 113, March 1959, pp. 1240-1253.
37. H. J. McSkimin and W. L. Bond, "Conical Refraction of Transverse Ultrasonic Waves in Quartz," *J. Acoust. Soc. Am.*, Vol. 39, March 1966, pp. 499-505.
38. R. A. Artman, "Ultrasonic Internal Conical Refraction in Potassium Chloride," *J. Acoust. Soc. Am.*, Vol. 39, March 1966, pp. 493-498.

39. R. E. Green, Jr., "Ultrasonic Investigation of Mechanical Properties," in Treatise on Materials Science and Technology, Vol. 3, Academic Press, New York, 1973.
40. J. R. Neighbors, "Elastic Energy Flow in Crystals of General Symmetry," *J. Appl. Phys.*, Vol. 44, November 1973, pp. 4816-4823.
41. B. A. Auld, Acoustic Fields and Waves in Solids, Vols. I and II, Wiley, New York, 1973.
42. A. E. Fein and C. S. Smith, "The Polarization of Acoustic Waves in Cubic Crystals," *J. Appl. Phys.*, Vol. 23, November 1952, pp. 1212-1213.
43. J. J. Campbell and W. R. Jones, "Propagation of Piezoelectric Surface Waves on Cubic and Hexagonal Crystals," *J. Appl. Phys.*, Vol 41, June 1970, pp. 2796-2801.
44. F. I. Fedorov, Theory of Elastic Waves in Crystals, (Plenum, New York, 1968).
45. R. D. Mindlin and Applied Mechanics, (G. Herrmann, ed.) Pergamon, Oxford, 1974.
46. H. F. Tiersten, "Thickness Vibrations of Piezoelectric Plates," *J. Acoust. Soc. Amer.*, Vol. 35, January 1963, pp. 53-58.
47. H. F. Tiersten, Linear Piezoelectric Plate Vibrations: Elements of the Linear Theory of Piezoelectricity and the Vibrations of Piezoelectric plates, (Plenum, New York, 1969).
48. T. Yamada and N. Niizeki, "Admittance of Piezoelectric Plates Vibrating Under the Perpendicular Field Excitation," *Proc. IEEE* Vol. 58, June 1970, pp. 941-942.
49. A. C. Lynch, "Measurement of the Equivalent Electrical Circuit of a Piezoelectric Crystal," *Proc. Phys. Soc. (London)*, Vol. 63B, 1950, pp. 323-331.
50. G. E. Martin, "Determination of Equivalent-Circuit Constants of Piezoelectric Resonators of Moderately Low Q by Absolute-Admittance Measurements," *J. Acoust. Soc. Am.*, Vol. 26, May 1954, pp. 413-420.
51. R. M. Glaister, "Measurement of Coupling Coefficient and Q of Low-Q Piezoelectric Ceramics," *Br. J. Appl. Phys.*, Vol 11, August 1960, pp. 390-391.
52. K. Shibayama, "Measurement of Small Values of Electromechanical - Coupling Coefficient in Piezoelectric Transducers," *J. Acoust. Soc. Am.*, Vol. 34, December 1962, pp. 1883-1886.

53. R. Holland, "Representation of Dielectric, Elastic, and Piezoelectric Losses by Complex Coefficients," IEEE Trans. on Sonics and Ultrasonics, Vol. SU-14, January 1967, pp. 18-20.
54. R. Holland and E. P. EerNisse, "Accurate Measurement of Coefficients in a Ferroelectric Ceramic," IEEE Trans. Sonics Ultrason., Vol SU-16, October 1969, pp. 173-181.
55. R. J. Zeto, C. G. Thornton, E. Hryckowian, and C. D. Bosco, "Low Temperature Thermal Oxidation of Silicon by Dry Oxygen Pressure above 1 Atm," J. Electrochem. Soc., Vol. 122, October 1975, pp. 1409-1410.
56. A. Ballato, "Resonance in Piezoelectric Vibrators," Proc. IEEE, Vol. 58, January 1970, pp. 149-151.
57. G. K. Guttwein, T. J. Lukaszek, and A. Ballato, "Practical Consequences of Modal Parameter Control in Crystal Resonators," USAECOM Technical Report ECOM-2847, June 1967, 21 pp.
58. F. K. Priebe and A. Ballato, "Comparison of Various Methods Used for Determination of Quartz Crystal Parameters in the Frequency Range 1 to 30 Mc," Proc. 18th Annual Frequency Control Symposium, Fort Monmouth, NJ, May 1964, pp. 458-486.
59. W. H. Horton and S. B. Boor, "Comparison of Crystal Measurement Equipment," Proc. 19th Annual Frequency Control Symposium, Fort Monmouth, NJ, April 1965, pp. 436-468.
60. F. K. Priebe and A. Ballato, "Measurement of Mode Parameters by Sweep Frequency Methods in the Frequency Range from 20 to 250 MHz," Proc. 20th Annual Frequency Control Symposium, Fort Monmouth, NJ, April 1966, pp. 465-499.
61. F. K. Priebe, "Filter Crystal Parameter Measurements with Frequency Modulated Signals (Sweep Frequency Methods): Frequency Range 1 MHz to 350 MHz," USAECOM Technical Report ECOM-2845, June 1967, 98 pp.
62. IRE Standards on Piezoelectric Crystals - The Piezoelectric Vibrator: Definitions and Methods of Measurement, 1957," Proc. IRE, Vol. 45, March 1957, pp. 353-358.
63. "Standard Definitions and Methods of Measurement for Piezoelectric Vibrators," IEEE Standard No. 177, May 1966, (Inst. of Elec. and Elx. Engrs., New York, 1966).
64. G. Sauerbrey, "Verwendung von Schwingquarzen zur Wägung dünner Schichten und zur Mikrowägung," Z. Physik, Vol. 155, 1959, pp. 206-222.

65. C. D. Stockbridge, "Resonance Frequency versus Mass Added to Quartz Crystals," *Vacuum Microbalance Techniques*, Vol. 5, 1966, pp. 193-205.
66. B. W. Kington, "The Quartz Crystal Microbalance," *Marconi Instrumentation*, Vol. 10, September 1966, pp. 81-84.
67. H. K. Pulker, "Factors Influencing the Accuracy of a Quartz-Crystal-Oscillator as a Thickness Monitor for Thin Film Deposition," *Thin Solid Films*, Vol. 1, 1967/1968, pp. 400-402.
68. D. R. Denison, "Linearity of a Heavily Loaded Quartz Crystal Microbalance," *J. Vac. Sci. Technol.*, Vol. 10, January/February 1973, pp. 126-129.
69. J.J. Campbell and W.R. Jones, "Propagation of Piezoelectric Surface Waves on Cubic and Hexagonal Crystals", *J. Appl. Phys.*, Vol. 41, June 1970, pp. 2796-2801.
70. S. Tamura and T. Sakuma, "Amplification of GHz Surface-Mode Acoustic Waves in a Piezoelectric Semiconductor Film", *Proc. IEEE Ultrason. Symp.*, October 1977, pp. 301-304.
71. D. Penunuri and K.M. Lakin, "Leaky Surface Wave Propagation on Si, GaAs, GaP, Al<sub>2</sub>O<sub>3</sub> and Quartz", *Proc. IEEE Ultrason. Symp.*, September 1975, pp. 478-483.
72. H. Gilboa, M.E. Motamedi and P. Das, "Study of GaAs Epitaxial Layer Using the Separated-Medium Acoustoelectric Effect", *Proc. IEEE Ultrason. Symp.*, September 1975, pp. 663-667.
73. M.J. Hoskins, S. Datta, C.M. Panasiak, and B.J. Hunsinger, "Line Acoustic Waves on Cleaved Edges in LiNbO<sub>3</sub> and GaAs", *Proc. IEEE Ultrason. Symp.*, September 1978, pp. 647-650.
74. C. - C. Tseng, "Piezoelectric Surface Waves in Cubic Crystals", *J. Appl. Phys.*, Vol. 41, May 1970, pp. 2270-2276.
75. V. Narayanamurti, R.A. Logan, M.A. Chin, and M. Lax, "Anisotropic Phonon Generation in GaAs Epilayers and pn Junctions", *Solid State Electron.*, Vol. 21, 1978, pp.1295-1298.
76. T.R. AuCoin, R.L. Ross, M.J. Wade, and R.O. Savage, "Liquid Encapsulated Compounding and Czochralski Growth of Semi-Insulating Gallium Arsenide", *Solid State Technol.*, Vol. 22, January 1979, pp. 59-62,67.
77. W.J. Fleming and J.E. Rowe, "Acoustoelectric Interactions in III-V Compound Semiconductors", In *Advances in Electronics and Electron Physics*, (L. Marton, ed.), Vol. 31, pp. 161-245, New York: Academic, 1972.
78. W.F. Boyle and R.J. Sladek, "Piezoelectric Stiffening and Attenuation of Ultrasonic Waves in n-Type GaSb Doped with Sulfur", *Phys. Rev. B*, Vol. 12, 15 July 1975, pp. 673-679.